Electronic Supplementary Material (ESI) for Environmental Science: Processes & Impacts.
This journal is © The Royal Society of Chemistry 2023

Electronic Supplementary Information for: Limitations of conventional approaches to identify photochemically produced reactive intermediates involved in contaminant indirect photodegradation

*Reid P. Milstead[1], Stephanie M. Berg[1], Bella M. Kelly[2], Christian D. Knellwolf[2], Cooper J. Larson[2], Kristine H. Wammer[2], and Christina K. Remucal[1,3]**

[1]Environmental Chemistry and Technology Program
University of Wisconsin – Madison
Madison, Wisconsin 53706

[2]Department of Chemistry
University of St. Thomas
St. Paul, Minnesota 55105

[3]Department of Civil and Environmental Engineering
University of Wisconsin – Madison
Madison, Wisconsin 53706

Contents (35 pages): Figures S1-S11 & Tables S1-S11

*Corresponding author address: 660 N. Park St., Madison, WI 53706;

email: remucal@wisc.edu; telephone: (608) 262-1820; fax: (608) 262-0454; Twitter: @remucal

Table of Contents

Section S1: Materials

Hydrochloric acid (concentrated, ACS grade), acetonitrile (HPLC grade), methanol (HPLC grade), and potassium hydrogen phthalate (ACS grade) were purchased from Fisher Scientific. Monobasic potassium phosphate (reagent grade), dibasic potassium phosphate (reagent grade), sodium terephthalate (>98%), sodium hydroxide (reagent grade), carbamazepine (>98%), sulfadiazine (>99%), potassium sorbate (>99%), isopropanol (>99.5%), 1,4-diazobicyclo[2,2,2]octane (DABCO; >99%), boric acid (100%), disodium tetraborate decahydrate (borax; 100%), and histidine (98%) were purchased from Sigma Aldrich. Formic acid (88% v/v, ACS grade) was purchased from Aqua Solutions. *para*-Nitroanisole (>99%) and sodium hypochlorite were purchased from Acros Organics. Pyridine (>99%) and 2,2′-azino-bis(3-ethyl-6-benzothiazolinesulfonate) (ABTS; 98%) were purchased from Alfa Aesar. Furfuryl alcohol (>98%) was purchased from Tokyo Chemical Industry. Atorvastatin (>95%) was purchased from Matrix Scientific. Benzotriazole (98%) was purchased from TCI America. Ultrapure water (18.2 MΩ cm) was obtained from a Milli-Q water purification system. Sodium hypochlorite was standardized using a Shimadzu UV-visible spectrometer ($\varepsilon_{292} = 359$ M^{-1} cm^{-1}).[1] All other materials were used as received.

Section S2: Sample collection

Water samples were collected from five different geographic areas (Northern Lakes, Mankato, St. Louis River, Yahara, and Twin Cities).[2] All of the wastewater samples were grouped into their own water category (i.e., ‘wastewater’), while the natural waters from each area make up their own respective water categories. The lake samples were collected from near the middle of each body of water via boat (top 1 m of the water column). River and ditch samples were collected by wading into each water. All samples were filtered through 0.45 µm nylon filters within 36 hours of sample collection and stored at 4 ^{o}C in the dark until analysis.

Seven natural water samples were collected from the North Temperate Lakes-Long Term Ecological Research (NTL-LTER) sites in northern Wisconsin and are labelled as the ‘Northern Lakes’ samples. These lakes include two dystrophic lakes (Crystal Bog and Trout Bog), one mesotrophic lake (Allequash Lake), and four oligotrophic lakes (Big Muskellunge Lake, Crystal Lake, Sparkling Lake, and Trout Lake).

Eight samples were collected near Mankato, Minnesota. The natural waters from this geographic area are labelled as the ‘Mankato’ samples. These samples include two agricultural ditches (Wammer Ditch, Olsen Ditch) and three river samples (Memories, Kiwannis, Seven-mile Creek). Memories and Kiwannis were in the Minnesota River and located upstream and downstream, respectively, of the Mankato Water Resource Recovery Facility (WRRF) samples. Three WRRF effluent samples were collected following secondary treatment. The WRRF pre-Cl sample was collected prior to disinfection, while the WRRF post-Cl sample was collected after chlorination and dechlorination with sodium bisulfite. The WRRF Reuse sample was chlorinated, but not dechlorinated.

A total of ten samples were collected in the Yahara watershed in Wisconsin. The natural waters are labelled as the ‘Yahara’ samples and include three physically connected lakes (Lake Mendota, Lake Wingra, Lake Kegonsa) and five river and stream samples (North Yahara, South Yahara, Confluence, Badfish upstream, Badfish downstream). Wastewater samples were collected from the Madison Metropolitan Sewerage District Nine Springs Wastewater Treatment Plant upstream (Nine Springs Pre-UV) and downstream (Nine Springs Post-UV) of UV disinfection.

Eleven samples were collected near the St. Louis River and Estuary in Duluth, MN and Superior, WI. The natural waters from this geographic area are labelled as the 'St. Louis River' samples and include seven river samples (Sand Creek, Meadowlands, River Inn, Munger Landing, East Detroit, Wisconsin Point, Blatnik Bridge). Four samples were collected from the Western Lake Superior Sanitary District (WLSSD) treatment plant. Samples were collected before (WLSSD Pre-Cl) and after (WLSSD post-Cl) disinfection by chlorine and dechlorination with sodium bisulfite during normal operations. Additional samples were collected before (WLSSD Influent) and after (WLSSD Effluent) chlorination/dechlorination when local paper mills were shut off.

Twelve samples were collected near the Twin Cities in Minnesota. The natural waters from this geographic area are labelled as the 'Twin Cities' samples and include five river samples (River Front Park, East River Parkway, Minnesota River, Metro Downstream, Eagle's Point Downstream) and three oligotrophic lakes (Lake of the Isles, Vadnais Lake, Lake Phalen). Effluent was collected from the Metropolitan Wastewater Treatment Plant (Metro WWTP) after secondary treatment (pre-Cl) and after chlorination and dechlorination with sodium bisulfite (post-Cl), and from Eagles WWTP after secondary treatment (pre-UV) and after following disinfection with UV light (post-UV).

Table S1. Names, date of collection, coordinates, and brief descriptions for all samples analyzed in this study. Samples are organized into the water groupings used in analysis.

Sample	Date	Coordinates	Description
Northern Lakes			
Crystal Bog (N1)	August 29, 2018	46.00800, -89.60570	Dystrophic lake
Trout Bog (N2)	August 29, 2018	46.04170, -89.68540	Dystrophic lake
Allequash Lake (N3)	August 30, 2018	46.04810, -89.61240	Mesotrophic lake

Big Muskellunge Lake (N4)	August 30, 2018	46.02730, -89.59350	Oligotrophic lake
Crystal Lake (N5)	August 30, 2018	45.9989, -89.60820	Oligotrophic lake
Sparkling Lake (N6)	August 28, 2018	46.01580, -89.69450	Oligotrophic lake
Trout Lake (N7)	August 30, 2018	46.07900, -89.64640	Oligotrophic lake
Mankato			
Memories (M1)	June 24, 2019	44.15543, -94.04223	Minnesota River; upstream of WRRF discharge
Olsen Ditch (M2)	June 25, 2019	44.11394, -94.26897	Agricultural ditch
Wammer Ditch (M3)	June 25, 2019	44.13387, -94.30944	Agricultural ditch
Seven-mile Creek (M4)	June 24, 2019	44.26217, -94.02657	Tributary to Minnesota River
Kiwannis (M5)	June 24, 2019	44.200262, -94.01779	Minnesota River, downstream of WRRF discharge
Yahara			
North Yahara (Y1)	July 26, 2019	43.156742 -89.343755	River that flows in Lake Mendota
Lake Mendota (Y2)	July 25, 2019	43.11294, -89.42145	Eutrophic lake
Lake Wingra (Y3)	October 9, 2019	43.053768, -89.419910	Eutrophic lake
Lake Kegonsa (Y4)	October 9, 2019	42.963891, -89.254772	Eutrophic lake
South Yahara (Y5)	July 26, 2019	42.94137, -89.20235	Yahara River; downstream of Lake Kegonsa
Badfish Upstream (Y6)	September 18, 2019	42.849748, -89.255665	Badfish Creek; upstream of MMSD discharge
Badfish Downstream (Y7)	September 18, 2019	42.849213, -89.255536	Badfish Creek; downstream of MMSD discharge
Confluence (Y8)	July 26, 2019	42.82017, -89.16300	Yahara River; downstream of confluence with Badfish Creek
St. Louis River			
Sand Creek (S1)	September 3, 2020	47.185510, -92.853331	Tributary to St. Louis River
Meadowlands (S2)	September 3, 2020	47.068966, -92.775002	St. Louis River

River Inn (S3)	September 3, 2020	46.702892, -92.418854	St. Louis River
Munger Landing (S4)	September 3, 2020	46.700820, -92.207148	St. Louis River
East Detroit (S5)	September 3, 2020	46.651824, -92.203205	St. Louis River
Blatnik Bridge (S6)	September 2, 2020	46.751031, -92.102092	St. Louis River Estuary
Wisconsin Point (S7)	September 2, 2020	46.688643, -91.972299	Shore of Lake Superior
Twin Cities			
River Front Park (T1)	August 27, 2020	45.06769, -93.28108	Minnesota River
East River Parkway (T2)	August 27, 2020	44.9579, -93.21307	Minnesota River
Minnesota River (T3)	August 27, 2020	44.88484, -93.17476	Minnesota River
Metro Downstream (T4)	August 31, 2020	44.88195, -93.01738	Minnesota River; downstream of Metro WWTP discharge
Eagles Point Downstream (T5)	August 31, 2020	44.74611, -92.85624	Minnesota River; downstream of Eagles Point WWTP discharge
Lake of the Isles (T6)	August 27, 2020	44.95174, -93.30727	Oligotrophic lake
Vadnais Lake (T7)	August 27, 2020	45.05128, -93.09446	Oligotrophic lake
Lake Phalen (T8)	August 27, 2020	44.98705, -93.05589	Oligotrophic lake
Wastewaters			
WRRF pre-Cl (W1)	June 24, 2019	44.18249, -94.00132	Final effluent before chlorination
WRRF Reuse (W2)	June 24, 2019	44.18249, -94.00132	Post chlorination/ dechlorination, used to cool plant
WRRF post-Cl (W3)	June 24, 2019	44.18249, -94.00132	Final effluent chlorination/post chlorination
Nine Springs Pre-UV (W4)	July 30, 2019	43.03967, -89.35752	Effluent collected before UV disinfection
Nine Springs Post-UV (W5)	July 30, 2019	43.03967, -89.35752	Effluent collected before UV disinfection
WLSSD Influent (W6)	May 6, 2020	46.761325, -92.124443	WLSSD effluent collected during local paper mill shutdown, pre-chlorination

WLSSD Effluent (W7)	May 6, 2020	46.761325, -92.124443	WLSSD effluent collected during local paper mill shutdown, post- chlorination/ dechlorination
WLSSD Pre-Cl (W8)	September 3, 2020	46.761325, -92.124443	WLSSD effluent pre-chlorination
WLSSD Post-Cl (W9)	September 3, 2020	46.761325, -92.124443	WLSSD effluent, post-chlorination/ dechlorination
Metro WWTP Pre-Cl (W10)	August 31, 2020	44.92612, -93.04823	Effluent collected pre-chlorination
Metro WWTP Post-Cl (W11)	August 31, 2020	44.92569, -93.04829	Effluent collect post chlorination/dechlorination
Eagles Point Pre-UV (W12)	August 31, 2020	44.78602, -92.91925	Effluent collected pre- UV disinfection
Eagles Point Post-UV (W13)	August 31, 2020	44.78602, -92.91925	Effluent collected post UV chlorination

Section S3: Bulk water chemistry

Table S2. Sample pH and concentrations of dissolved organic carbon (DOC), dissolved inorganic carbon (DIC), iron (Fe), and nitrate (NO_3^-). Nitrite was not detected in any water sample.

Sample	pH	[DOC] (mg-C L^{-1})	[DIC] (mg-C L^{-1})	[Fe] (mg L^{-1})	[NO_3^-] (mg L^{-1})
Northern Lakes					
Crystal Bog (N1)	7.5 ± 0.1	11.0 ± 0.1	4.0 ± 0.4	< 0.1	< 0.5
Trout Bog (N2)	7.5 ± 0.1	23.7 ± 0.4	1.4 ± 0.1	0.3 ± 0.1	< 0.5
Allequash Lake (N3)	8.4 ± 0.1	5.0 ± 0.1	10.2 ± 0.1	0.7 ± 0.2	< 0.5
Big Muskellunge Lake (N4)	7.9 ± 0.1	4.2 ± 0.1	6.0 ± 0.5	< 0.1	< 0.5
Crystal Lake (N5)	7.0 ± 0.1	2.6 ± 0.1	1.4 ± 0.1	< 0.1	< 0.5
Sparkling Lake (N6)	8.1 ± 0.1	3.4 ± 0.1	10.7 ± 0.1	< 0.1	< 0.5
Trout Lake (N7)	7.9 ± 0.1	3.0 ± 0.2	10.7 ± 0.1	< 0.1	< 0.5
Mankato					
Memories (M1)	8.5 ± 0.1	4.6 ± 0.1	63.4 ± 0.1	< 0.1	18.0 ± 0.1
Olsen Ditch (M2)	8.3 ± 0.1	1.8 ± 0.1	77.2 ± 0.2	< 0.1	44.4 ± 0.2
Wammer Ditch (M3)	8.4 ± 0.1	3.3 ± 0.1	68.4 ± 0.1	< 0.1	32.3 ± 0.1
Seven-mile Creek (M4)	8.5 ± 0.1	3.9 ± 0.1	66.8 ± 0.1	< 0.1	42.2 ± 0.1
Kiwannis (M5)	8.4 ± 0.1	4.3 ± 0.1	62.8 ± 0.2	< 0.1	21.4 ± 0.1

Yahara					
North Yahara (Y1)	8.4 ± 0.1	4.7 ± 0.1	62.6 ± 0.1	< 0.1	11.3 ± 0.1
Lake Mendota (M2)	8.7 ± 0.1	3.8 ± 0.1	37.4 ± 0.1	< 0.1	< 0.5
Lake Wingra (M3)	8.5 ± 0.1	4.3 ± 0.1	41.2 ± 0.1	< 0.1	< 0.5
Lake Kegonsa (M4)	8.4 ± 0.1	10.5 ± 0.1	41.0 ± 0.1	< 0.1	< 0.5
South Yahara (M5)	8.4 ± 0.1	7.1 ± 0.1	46.8 ± 0.2	< 0.1	0.8 ± 0.1
Badfish Upstream (M6)	8.5 ± 0.1	2.4 ± 0.1	62.0 ± 0.2	< 0.1	14.1 ± 0.1
Badfish Downstream (M7)	8.4 ± 0.1	4.4 ± 0.6	68.4 ± 0.3	< 0.1	72.5 ± 0.5
Confluence (M8)	8.4 ± 0.1	4.1 ± 0.1	54.8 ± 0.3	< 0.1	10.2 ± 0.1
St. Louis River					
Sand Creek (S1)	7.7 ± 0.1	69 ± 6	7.5 ± 0.1	5.9 ± 0.1	< 0.5
Meadowlands (S2)	8.1 ± 0.1	28.4 ± 0.8	30 ± 1	1.9 ± 0.1	< 0.5
River Inn (S3)	8.2 ± 0.1	24.8 ± 0.8	20.1 ± 0.1	1 ± 0.1	< 0.5
Munger Landing (S4)	8.2 ± 0.1	23.1 ± 0.5	18.2 ± 0.1	0.7 ± 0.1	< 0.5
East Detroit (S5)	8.2 ± 0.1	24.2 ± 0.1	18.4 ± 0.1	0.7 ± 0.1	< 0.5
Blatnik Bridge (S6)	8.4 ± 0.1	18 ± 5	20.8 ± 0.1	0.3 ± 0.1	1.1 ± 0.1
Wisconsin Point (S7)	8.3 ± 0.1	8 ± 1	11.0 ± 0.1	< 0.1	1.2 ± 0.1
Twin Cities					
River Front Park (T1)	8.3 ± 0.1	31 ± 4	36.6 ± 0.2	< 0.1	0.8 ± 0.1
East River Parkway (T2)	8.4 ± 0.1	18 ± 9	35.7 ± 0.2	< 0.1	0.5 ± 0.1
Minnesota River (T3)	8.4 ± 0.1	5.2 ± 0.5	53.7 ± 0.2	< 0.1	16.7 ± 0.1
Metro Downstream (T4)	8.4 ± 0.1	9.0 ± 0.1	41.7 ± 0.2	< 0.1	4.4 ± 0.1
Eagles Point Downstream (T5)	8.4 ± 0.1	8.9 ± 0.4	38.4 ± 0.3	< 0.1	5.4 ± 0.1
Lake of the Isles (T6)	8.5 ± 0.1	8.7 ± 0.3	23.5 ± 0.1	< 0.1	< 0.5
Vadnais Lake (T7)	8.5 ± 0.1	7.5 ± 0.4	28.1 ± 0.1	< 0.1	< 0.5

Lake Phalen (T8)	8.5 ± 0.1	6.7 ± 0.2	26.8 ± 0.1	< 0.1	< 0.5
Wastewaters					
WRRF Pre-Cl (W1)	8.2 ± 0.1	4.8 ± 0.5	43.2 ± 0.3	< 0.1	70.9 ± 0.5
WRRF Reuse (W2)	8.3 ± 0.1	6.4 ± 1	44.4 ± 0.2	< 0.1	90.2 ± 0.5
WRRF Post-Cl (W3)	8.3 ± 0.1	5.0 ± 0.3	43.5 ± 0.2	< 0.1	86.2 ± 0.5
Nine Springs PreUV (W4)	8.4 ± 0.1	5.3 ± 0.1	67.8 ± 0.3	< 0.1	76.4 ± 0.5
Nine Springs PostUV (W5)	8.6 ± 0.1	5.9 ± 0.3	66.9 ± 0.4	< 0.1	77.9 ± 0.5
WLSSD Influent (W6)	7.3 ± 0.1	29 ± 2	65 ± 1	0.5 ± 0.1	< 0.5
WLSSD Effluent (W7)	8.1 ± 0.1	24 ± 2	72.0 ± 0.3	0.4 ± 0.1	< 0.5
WLSSD Pre-Cl (W8)	8.2 ± 0.1	53 ± 5	88.8 ± 0.6	0.9 ± 0.1	0.5 ± 0.3
WLSSD Post-Cl (W9)	8.3 ± 0.1	43 ± 6	92.7 ± 0.4	1.0 ± 0.1	< 0.5
Metro WWTP Pre-Cl (W10)	8.3 ± 0.1	8.2 ± 0.8	53.1 ± 0.4	< 0.1	6.8 ± 0.3
Metro WWTP Post-Cl (W11)	8.3 ± 0.1	9 ± 1	46.8 ± 0.4	< 0.1	63 ± 1
Eagles Point Pre-UV (W12)	8.2 ± 0.1	7.5 ± 0.7	42.0 ± 0.3	< 0.1	109 ± 1
Eagles Point Post-UV (W13)	8.2 ± 0.1	9 ± 2	42.6 ± 0.1	< 0.1	111 ± 1

Table S3. Optical parameters and electron donating capacities of each of the samples.

Sample	**$SUVA_{254}$ (L mg-C^{-1} m^{-1})**	**E_2:E_3**	**HIX**	**FI**	**EDC (mmol e^- g-C^{-1})**
Northern Lakes					
Crystal Bog (N1)	2.16	5.79	1.17	1.43	2.34 ± 0.2
Trout Bog (N2)	2.89	5.79	0.53	1.43	2.85 ± 0.7
Allequash Lake (N3)	1.92	7.56	0.51	1.50	1.63 ± 0.2
Big Muskellunge Lake (N4)	0.47	8.75	0.31	1.53	0.26 ± 0.4
Crystal Lake (N5)	0.25	8.58	0.73	1.54	0.66 ± 0.2
Sparkling Lake (N6)	1.08	9.69	0.35	1.60	0.76 ± 0.06
Trout Lake (N7)	0.81	9.72	0.47	1.51	0.71 ± 0.09
Mankato					

Memories (M1)	2.60	9.5	0.39	1.65	1.25 ± 0.2
Olsen Ditch (M2)	4.00	10.77	0.49	1.69	0.96 ± 0.03
Wammer Ditch (M3)	2.46	9.22	0.29	1.64	1.20 ± 0.2
Seven-mile Creek (M4)	3.11	7.7	0.33	1.70	1.83 ± 0.3
Kiwannis (M5)	2.56	7.97	0.52	1.61	1.16 ± 0.2
Yahara					
North Yahara (Y1)	2.94	7.5	0.45	1.60	2.04 ± 0.3
Lake Mendota (Y2)	1.58	10.46	0.40	1.68	0.76 ± 0.1
Lake Wingra (Y3)	2.03	8.24	0.74	1.61	1.54 ± 0.2
Lake Kegonsa (Y4)	1.23	5.68	3.18	1.61	0.68 ± 0.3
South Yahara (Y5)	1.35	7.1	0.21	1.64	0.78 ± 0.09
Badfish Upstream (Y6)	3.45	7.44	0.38	1.72	2.44 ± 0.2
Badfish Downstream (Y7)	2.34	5.98	0.54	2.00	4.36 ± 0.1
Confluence (Y8)	2.39	6.6	0.29	1.70	1.19 ± 0.2
St. Louis River					
Sand Creek (S1)	3.31	5.35	1.98	1.50	1.55 ± 0.6
Meadowlands (S2)	3.18	5.43	0.94	1.52	1.53 ± 0.8
River Inn (S3)	3.18	6.54	0.89	1.52	1.72 ± 0.7
Munger Landing (S4)	2.88	6.05	0.41	1.50	1.57 ± 0.7
East Detroit (S5)	2.97	5.94	0.55	1.51	1.64 ± 0.6
Blatnik Bridge (S6)	2.13	6.34	0.00	1.49	1.42 ± 0.3
Wisconsin Point (S7)	0.20	6.52	0.48	1.46	0.24 ± 0.02
Twin Cities					
River Front Park (T1)	0.82	7.54	0.41	1.53	0.50 ± 0.4
East River Parkway (T2)	4.72	13.05	0.52	1.55	0.45 ± 0.3
Minnesota River (T3)	2.28	7.12	0.41	1.60	1.03 ± 0.2
Metro Downstream (T4)	2.33	7.22	0.37	1.56	1.23 ± 0.4
Eagles Point Downstream (T5)	2.17	7.19	0.34	1.57	1.30 ± 0.4
Lake of the Isles (T6)	0.97	9.75	0.28	1.64	0.67 ± 0.2
Vadnais Lake (T7)	1.64	10.28	0.42	1.58	0.98 ± 0.3
Lake Phalen (T8)	1.3	10.97	0.32	1.60	0.76 ± 0.3
Wastewaters					
WRRF Pre-Cl (W1)	1.68	8.52	0.59	2.04	1.61 ± 0.3
WRRF Reuse (W2)	1.01	12.48	0.55	1.92	0.51 ± 0.3
WRRF Post-Cl (W3)	1.33	10.56	0.52	1.97	1.13 ± 0.4

Nine Springs Pre-UV (W4)	2.11	6.08	0.34	2.04	4.01 ± 0.4
Nine Springs Post-UV (W5)	1.72	5.96	0.57	2.03	3.21 ± 0.8
WLSSD Influent (W6)	2.18	5.98	0.62	1.74	5.3 ± 1
WLSSD Effluent (W7)	2.06	6.72	0.40	1.72	5.38 ± 0.7
WLSSD Pre-Cl (W8)	1.86	6.93	0.22	1.56	2.1 ± 1
WLSSD Post-Cl (W9)	2.34	7.06	0.52	1.54	2.43 ± 0.8
Metro WWTP Pre-Cl (W10)	1.51	5.84	0.41	1.98	2.01 ± 0.2
Metro WWTP Post-Cl (W11)	1.51	5.84	0.27	1.98	1.69 ± 0.2
Eagles Point Pre-UV (W12)	1.46	5.07	0.37	2.08	2.42 ± 0.3
Eagles Point Post-UV (W13)	2.17	7.19	0.48	2.09	2.0 ± 0.3

Section S4: FT-ICR MS analysis

Table S4. Total number of formula matches, average weighted H:C ($H:C_w$), average weighted O:C ($O:C_w$), and average weighted double bond equivalents (DBE_w) for all samples.

Sample	Total # formulas	$H:C_w$	$O:C_w$	DBE_w
Northern Lakes				
Crystal Bog (N1)	2691	1.11	0.53	9.67
Trout Bog (N2)	2172	1.09	0.55	9.93
Allequash Lake (N3)	3300	1.15	0.52	9.19
Big Muskellunge Lake (N4)	3716	1.28	0.51	7.78
Crystal Lake (N5)	3231	1.36	0.49	6.65
Sparkling Lake (N6)	3960	1.23	0.49	8.41
Trout Lake (N7)	3555	1.23	0.51	8.42
Mankato				
Memories (M1)	4267	1.16	0.52	9.49
Olsen Ditch (M2)	3300	1.15	0.51	9.79
Wammer Ditch (M3)	4290	1.17	0.50	9.30
Seven-mile Creek (M4)	4176	1.15	0.51	9.63
Kiwannis (M5)	4217	1.17	0.51	9.42
Yahara				
North Yahara (Y1)	4608	1.12	0.51	9.55

Lake Mendota (Y2)	4970	1.22	0.50	8.66
Lake Wingra (Y3)	4988	1.20	0.49	8.76
Lake Kegonsa (Y4)	5045	1.20	0.50	8.92
South Yahara (Y5)	5169	1.20	0.50	8.84
Badfish Upstream (Y6)	4852	1.20	0.48	9.02
Badfish Downstream (Y7)	5322	1.26	0.47	8.22
Confluence (Y8)	4955	1.18	0.51	9.03
St. Louis River				
Sand Creek (S1)	3057	1.28	0.41	7.81
Meadowlands (S2)	3047	1.33	0.38	7.19
River Inn (S3)	3266	1.26	0.43	8.05
Munger Landing (S4)	3124	1.29	0.40	7.68
East Detroit (S5)	3029	1.32	0.39	7.39
Blatnik Bridge (S6)	3338	1.35	0.37	6.96
Wisconsin Point (S7)	2150	1.60	0.20	4.52
Twin Cities				
River Front Park (T1)	3601	1.34	0.38	7.09
East River Parkway (T2)	3822	1.43	0.30	6.22
Minnesota River (T3)	3477	1.49	0.30	5.55
Metro Downstream (T4)	4028	1.41	0.33	6.48
Eagles Point Downstream (T5)	4055	1.47	0.28	5.83
Lake of the Isles (T6)	4422	1.51	0.28	5.47
Vadnais Lake (T7)	4038	1.45	0.31	6.07
Lake Phalen (T8)	4419	1.46	0.30	5.89
Wastewaters				
WRRF Pre-Cl (W1)	4772	1.27	0.48	8.10
WRRF Reuse (W2)	4336	1.29	0.48	7.75
WRRF Post-Cl (W3)	4689	1.28	0.49	7.97
Nine Springs Pre-UV (W4)	5155	1.34	0.51	7.26
Nine Springs Post-UV (W5)	5047	1.35	0.49	7.15
WLSSD Influent (W6)	3245	1.40	0.40	6.66
WLSSD Effluent (W7)	4272	1.43	0.39	6.25
WLSSD Pre-Cl (W8)	3998	1.27	0.46	7.60
WLSSD Post-Cl (W9)	3878	1.33	0.43	7.09
Metro WWTP Pre-Cl (W10)	4842	1.51	0.29	5.32
Metro WWTP Post-Cl (W11)	4466	1.48	0.33	5.52
Eagles Point Pre-UV (W12)	4451	1.55	0.28	4.93
Eagles Point Post-UV (W13)	4417	1.54	0.28	4.96

Section S5: PPRI quantification

Probe compound quantification. The probe compounds furfuryl alcohol (FFA), terephthalic acid (TPA), and 2,4,6-trimethylphenol (TMP) were used in separate experiments to quantify the formation of singlet oxygen ($^1O_2$), hydroxyl radical ($^{\bullet}OH$), and triplet state DOM (^3DOM), respectively, in all water samples. Sample irradiation times varied to allow for four to five sampling points to be collected. For TPA, only the initial time points were used for calculations, as this probe quantifies the rate of formation of hydroxy-terephthalic acid (hTPA) instead of the first-order degradation of the probe compounds. At least three of the time points were included in the TPA measurements. Both FFA and TMP concentrations exhibited pseudo-first-order degradation kinetics over the experimental time frame. All reactions occurred at room temperature.

The formation of hTPA and the degradation of FFA, TMP, and the *p*-nitroanisole (PNA) actinometer were quantified using high-performance liquid chromatography (HPLC; equipped with 1260 diode array detector and a 1260 fluorescence detector).

Table S5. HPLC methods used to quantify the degradation of FFA, TMP, PNA, and the formation of hTPA.

Furfuryl alcohol (FFA)	
Pump settings	0.6 mL/min flow rate Isocratic: 90% 0.1% v/v formic acid, 10% ACN
Column	Agilent Poroshell 120 EC-C18 (3.0 x 50 mm) w/ guard column (3.0 mm)
Elution time	1.7 min
Wavelength	217 nm
2,4,6-Trimethylphenol (TMP)	
Pump settings	0.75 mL/min flow rate Isocratic: 50% 0.1% v/v formic acid, 50% ACN
Column	Agilent Poroshell 120 EC-C18 (3.0 x 50 mm) w/ guard column (3.0 mm)
Elution time	0.8 min
Wavelength	excitation: 315 nm, emission: 425 nm
***p*-Nitroanisole (PNA)**	
Pump settings	0.6 mL/min flow rate Isocratic: 50% 0.1% v/v formic acid, 50% ACN
Column	Agilent Poroshell 120 EC-C18 (3.0 x 50 mm) w/ guard column (3.0 mm)

Elution time	1.5 min
Wavelength	314 nm
hydroxy-terephthalic acid (hTPA)	
Pump settings	1.5 mL/min flow rate Isocratic: 60% 0.1% phosphoric acid, 40% ACN
Column	Agilent Poroshell 120 Bonus RP (3.0 x 100 mm) w/ guard column (3.0 mm)
Wavelength	excitation: 250 nm, emission: 410 nm

Steady-state concentrations. Steady-state concentrations of ^{3}DOM were calculated as described previously:[3]

$$[^3DOM]_{ss} = \frac{\Delta[TMP]/\Delta t}{k_{TMP}} \tag{S1}$$

where k_{obs} is the pseudo-first order observed rate constant of TMP degradation and k_{TMP} is the second order rate constant for the reaction between ^{3}DOM and TMP (2.6 x 10^{-9} M^{-1} s^{-1}).[3] Importantly, these experiments were conducted at a normalized [DOC] value of 5 mg-C L^{-1}. Steady-state concentrations of $^1O_2$ were determined based on the observed loss rate of FFA:[4]

$$[^1O_2]_{ss} = \frac{\Delta[FFA]/\Delta t}{k_{FFA}} \tag{S2}$$

where k_{FFA} is the rate constant for the reaction between $^1O_2$ and FFA (1.00 x 10^8 M^{-1} s^{-1}).[5] Steady-state concentrations for hydroxyl radical ($[^\bullet OH]_{ss}$) were determined as:

$$[^\bullet OH]_{ss} = \frac{\Delta[hTPA]/\Delta t}{k_{TPA}} \tag{S3}$$

where k_{TPA} is the rate constant for the reaction between hydroxyl radical and TPA (4.4 x 10^9 M^{-1} s^{-1}).[6]

Light intensity. The light intensity of irradiation experiments was determined using a calculated screening factor (*S*) and the rate of light absorbance (R_a). The screening factor at each wavelength was calculated using decadal absorbance (α_λ, cm^{-1}) and experimental pathlength (*l*, cm):

$$S_\lambda = \frac{1-10^{-l \times \alpha_\lambda}}{2.303 \times l \times \alpha_\lambda} \tag{S4}$$

The rate of light absorbance of the PNA actinomter ($R_{a,\ PNA}$) was calculated using the pseudo-first-order loss rate of PNA ($k_{obs,\ PNA}$, s^{-1}), the initial concentration of PNA ($[PNA]_{t=0}$, M), and the quantum yield of the reaction between PNA and pyridine (Φ_{PNA}):[7]

$$\sum_\lambda R_{a,PNA,\lambda} = \frac{k_{obs,PNA}[PNA]_{t=0}}{\Phi_{PNA}} \tag{S5}$$

R_a values were integrated from 315 – 415 nm. The photon flux was (I, E cm^{-2} s^{-1}) was then calculated as:

$$I = \sum_\lambda \frac{R_{a,PNA,\lambda}}{2.303 \times S_\lambda \times \varepsilon_\lambda \times l} \tag{S6}$$

where ε_λ is the molar absorptivity of PNA at a given wavelength.

Quantum yields of PPRI. The quantum yield of singlet oxygen formation (Φ_{1O2}) was calculated as described previously[4] using Φ_{PNA}, $[PNA]_{t=0}$, $k_{obs,\ PNA}$, the rate constant for quenching of $^1O_2$ by water (k_d, 2.4 x 10^5 s^{-1}),[3,5] k_{FFA}, the rate of light absorption of both PNA ($R_{a,\ PNA}$) and FFA ($R_{a,\ FFA}$), and the observed rate constant of degradation of FFA ($k_{obs,\ FFA}$):

$$\Phi_{1O2} = \frac{\Phi_{PNA}}{[PNA]_{t=0}} \times \frac{R_{a,PNA}}{R_{a,FFA}} \times \frac{(k_{obs,FFA} \times k_d)}{(k_{obs,PNA} \times k_{FFA})} \tag{S7}$$

The quantum yield coefficient of ^3DOM (f_{TMP}, M^{-1}) was calculated as described previously[8] using Φ_{PNA}, $[PNA]_{t=0}$, $k_{obs,\ PNA}$, $R_{a,\ PNA}$, and the rate of light absorption of TMP ($R_{a,\ TMP}$):

$$f_{TMP} = \frac{\Phi_{PNA}}{[PNA]_{t=0}} \times \frac{R_{a,PNA}}{R_{a,TMP}} \times \frac{k_{obs,TMP}}{k_{obs,PNA}} \tag{S8}$$

The quantum yield of hydroxyl radical ($\Phi_{\bullet OH}$) was calculated using $[^{\bullet}OH]_{ss}$, $R_{a,\ TPA}$, $[HCO_3^-]$, $[CO_3^{2-}]$, and [DOC]:[2,9,10]

$$\Phi_{\bullet OH} = \frac{k_{\bullet OH,HCO3}[HCO_3^-] + k_{\bullet OH,CO3}[CO_3^{2-}] + k_{\bullet OH,[DOC]}[DOC][\bullet OH]_{ss}}{R_a} \tag{S9}$$

where $k_{\bullet OH,HCO3}$ = 8.5 x 10^{6} M^{-1} s^{-1}, $k_{\bullet OH,CO3}$ = 3.9 x 10^{8} M^{-1} s^{-1}, and $k_{\bullet OH,DOM}$ = 1.9 x 10^{4} mg-C^{-1} L s^{-1}.[9,10]

Table S6. Quantum yields and/or quantum yield coefficients, as well as steady-state concentrations, for ^{3}DOM, $^{1}O_2$, and $^{\bullet}$OH. Error represents the standard deviation of triplicate measurements. Measurements of $\Phi_{\bullet OH}$ are not available for two of the wastewater samples due to fluorescence interference in these samples.

Sample	f_{TMP} (M^{-1})	Φ_{1O2}	$\Phi_{\bullet OH}$	[^{3}DOM]$_{ss}$ (M)	[$^{1}O_2$]$_{ss}$ (M)	[$^{\bullet}$OH]$_{ss}$ (M)
Northern Lakes						
Crystal Bog (N1)	11.6 ± 0.4	(1.4 ± 0.2) x 10^{-2}	(8 ± 1) x 10^{-5}	(3.2 ± 0.1) x 10^{-14}	(4.1 ± 0.5) x 10^{-13}	(3.8 ± 0.5) x 10^{-16}
Trout Bog (N2)	14.62 ± 0.03	(1.1 ± 0.1) x 10^{-2}	(1.2 ± 0.1) x 10^{-4}	(4.1 ± 0.1) x 10^{-14}	(8.4 ± 0.9) x 10^{-13}	(6.3 ± 0.6) x 10^{-16}
Allequash Lake (N3)	20.8 ± 0.7	(2.1 ± 0.1) x 10^{-2}	(4.6 ± 0.8) x 10^{-5}	(4.7 ± 0.2) x 10^{-14}	(2.0 ± 0.1) x 10^{-13}	(1.9 ± 0.4) x 10^{-16}
Big Muskellunge Lake (N4)	19.8 ± 0.4	(3.3 ± 0.6) x 10^{-2}	(5.0 ± 0.8) x 10^{-5}	(1.5 ± 0.1) x 10^{-14}	(9 ± 2) x 10^{-14}	(8 ± 1) x 10^{-17}
Crystal Lake (N5)	12.1 ± 0.9	(2.5 ± 0.3) x 10^{-2}	(4 ± 1) x 10^{-5}	(5.8 ± 0.4) x 10^{-15}	(4.3 ± 0.7) x 10^{-14}	(7 ± 2) x 10^{-17}
Sparkling Lake (N6)	26.5 ± 0.6	(2.5 ± 0.6) x 10^{-2}	(3.4 ± 0.2) x 10^{-5}	(2.6 ± 0.1) x 10^{-14}	(7.8 ± 0.9) x 10^{-14}	(8.8 ± 0.5) x 10^{-17}
Trout Lake (N7)	15.8 ± 0.7	(2.8 ± 0.2) x 10^{-2}	(3.2 ± 0.96) x 10^{-5}	(1.2 ± 0.1) x 10^{-14}	(7.4 ± 0.6) x 10^{-14}	(7 ± 2) x 10^{-17}
Mankato						
Memories (M1)	44 ± 2	(7.3 ± 0.3) x 10^{-2}	(4.5 ± 0.3) x 10^{-5}	(1.1 ± 0.1) x 10^{-13}	(4.2 ± 0.1) x 10^{-13}	(1.9 ± 0.2) x 10^{-16}
Olsen Ditch (M2)	55 ± 2	(4.6 ± 0.1) x 10^{-2}	(9.9 ± 0.2) x 10^{-5}	(1.0 ± 0.1) x 10^{-13}	(4.7 ± 0.6) x 10^{-13}	(6.1 ± 0.1) x 10^{-16}
Wammer Ditch (M3)	41.5 ± 0.8	(4.0 ± 0.1) x 10^{-2}	(5.7 ± 0.4) x 10^{-5}	(7.8 ± 0.2) x 10^{-14}	(3.1 ± 0.1) x 10^{-13}	(2.4 ± 0.2) x 10^{-16}
Seven-mile Creek (M4)	39.7 ± 0.1	(4.3 ± 0.1) x 10^{-2}	(3.4 ± 0.3) x 10^{-5}	(1.1 ± 0.1) x 10^{-13}	(4.7 ± 0.1) x 10^{-13}	(1.9 ± 0.2) x 10^{-16}
Kiwannis (M5)	47.3 ± 0.8	(4.4 ± 0.1) x 10^{-2}	(3.5 ± 0.2) x 10^{-5}	(1.1 ± 0.1) x 10^{-13}	(4.1 ± 0.1) x 10^{-13}	(1.5 ± 0.1) x 10^{-16}
Yahara						
North Yahara (Y1)	30.3 ± 0.3	(3.1 ± 0.1) x 10^{-2}	(2.7 ± 0.1) x 10^{-4}	(9.4 ± 0.1) x 10^{-14}	(4.3 ± 0.1) x 10^{-13}	(1.4 ± 0.1) x 10^{-15}
Lake Mendota (Y2)	39.1 ± 0.7	(2.8 ± 0.3) x 10^{-2}	(9.7 ± 0.2) x 10^{-6}	(6.2 ± 0.1) x 10^{-14}	(1.9 ± 0.2) x 10^{-13}	(3.2 ± 0.1) x 10^{-16}

Lake Wingra (Y3)	33 ± 1	(3.2 ± 0.1) x 10^{-2}	(5.6 ± 0.6) x 10^{-5}	(7.7 ± 0.3) x 10^{-14}	(3.2 ± 0.1) x 10^{-13}	(2.5 ± 0.2) x 10^{-16}
Lake Kegonsa (Y4)	56.6 ± 0.3	(5.3 ± 0.1) x 10^{-2}	(1.4 ± 0.1) x 10^{-4}	(6.2 ± 0.1) x 10^{-14}	(5.3 ± 0.1) x 10^{-13}	(2.6 ± 0.2) x 10^{-16}
South Yahara (Y5)	40.58 ± 0.08	(2.8 ± 0.2) x 10^{-2}	(2.7 ± 0.5) x 10^{-5}	(6.3 ± 0.1) x 10^{-14}	(2.7 ± 0.2) x 10^{-13}	(7 ± 1) x 10^{-17}
Badfish Upstream (Y6)	45 ± 1	(3.8 ± 0.1) x 10^{-2}	(4.3 ± 0.1) x 10^{-5}	(9.1 ± 0.3) x 10^{-14}	(2.9 ± 0.1) x 10^{-13}	(2.4 ± 0.1) x 10^{-16}
Badfish Downstream (Y7)	41 ± 2	(2.8 ± 0.1) x 10^{-2}	(1.1 ± 0.2) x 10^{-4}	(7.8 ± 0.2) x 10^{-14}	(3.0 ± 0.1) x 10^{-13}	(5 ± 1) x 10^{-16}
Confluence (Y8)	47.3 ± 0.5	(2.4 ± 0.9) x 10^{-2}	(3.0 ± 0.8) x 10^{-5}	(8.6 ± 0.1) x 10^{-14}	(1.8 ± 0.4) x 10^{-13}	(1.0 ± 0.3) x 10^{-16}
St. Louis River						
Sand Creek (S1)	23 ± 5	(6 ± 1) x 10^{-3}	(5.8 ± 0.1) x 10^{-4}	(4.2 ± 1.0) x 10^{-14}	(8 ± 1) x 10^{-13}	(2.0 ± 0.1) x 10^{-15}
Meadowlands (S2)	30 ± 2	(1.1 ± 0.1) x 10^{-2}	(1.4 ± 0.1) x 10^{-4}	(8.6 ± 0.5) x 10^{-14}	(6.0 ± 0.1) x 10^{-13}	(7.2 ± 0.1) x 10^{-16}
River Inn (S3)	31 ± 3	(1.4 ± 0.1) x 10^{-2}	(1.3 ± 0.1) x 10^{-4}	(8.7 ± 0.8) x 10^{-14}	(6.1 ± 0.1) x 10^{-13}	(6.5 ± 0.1) x 10^{-16}
Munger Landing (S4)	31.0 ± 0.5	(1.7 ± 0.1) x 10^{-2}	(7.1 ± 0.2) x 10^{-5}	(8.4 ± 0.1) x 10^{-14}	(6.4 ± 0.4) x 10^{-13}	(3.5 ± 0.1) x 10^{-16}
East Detroit (S5)	30.3 ± 0.1	(1.6 ± 0.1) x 10^{-2}	(8.4 ± 0.1) x 10^{-5}	(8.2 ± 0.1) x 10^{-14}	(6.3 ± 0.1) x 10^{-13}	(4.2 ± 0.1) x 10^{-16}
Blatnik Bridge (S6)	27 ± 2	(1.8 ± 0.1) x 10^{-2}	(6.8 ± 0.2) x 10^{-5}	(5.9 ± 0.4) x 10^{-14}	(5.2 ± 0.3) x 10^{-13}	(2.7 ± 0.1) x 10^{-16}
Wisconsin Point (S7)	14 ± 2	(2.3 ± 0.1) x 10^{-2}	(1.4 ± 0.1) x 10^{-4}	(5.9 ± 0.9) x 10^{-15}	(4.9 ± 1.0) x 10^{-14}	(1.1 ± 0.1) x 10^{-16}
Twin Cities						
River Front Park (T1)	61.1 ± 0.7	(4.7 ± 0.1) x 10^{-2}	(1.9 ± 0.1) x 10^{-4}	(4.3 ± 0.1) x 10^{-14}	(6.7 ± 0.1) x 10^{-13}	(2.6 ± 0.1) x 10^{-16}
East River Parkway (T2)	50 ± 2	(3.2 ± 0.1) x 10^{-2}	(1.1 ± 0.1) x 10^{-5}	(6.3 ± 0.2) x 10^{-14}	(4.7 ± 0.1) x 10^{-13}	(2.7 ± 0.1) x 10^{-16}
Minnesota River (T3)	87.1 ± 0.5	(5.9 ± 0.1) x 10^{-2}	(2.4 ± 0.1) x 10^{-4}	(1.2 ± 0.1) x 10^{-13}	(4.1 ± 0.1) x 10^{-13}	(8.7 ± 0.4) x 10^{-16}
Metro Downstream (T4)	37.8 ± 0.7	(3.7 ± 0.6) x 10^{-2}	(1.1 ± 0.1) x 10^{-4}	(8.6 ± 0.1) x 10^{-14}	(5 ± 1) x 10^{-13}	(4.2 ± 0.3) x 10^{-16}
Eagles Point Downstream (T5)	26.8 ± 0.5	(3.7 ± 0.1) x 10^{-2}	(1.3 ± 0.1) x 10^{-4}	(8.7 ± 0.5) x 10^{-14}	(4.8 ± 0.1) x 10^{-13}	(4.7 ± 0.2) x 10^{-16}
Lake of the Isles (T6)	78 ± 3	(5.8 ± 0.3) x 10^{-2}	(5.3 ± 0.9) x 10^{-5}	(5.6 ± 0.2) x 10^{-14}	(2.4 ± 0.1) x 10^{-13}	(7 ± 1) x 10^{-17}
Vadnais Lake (T7)	60 ± 3	(4.7 ± 0.1) x 10^{-2}	(3.4 ± 0.3) x 10^{-5}	(7.4 ± 0.3) x 10^{-14}	(2.9 ± 0.1) x 10^{-13}	(7.5 ± 0.5) x 10^{-17}

Lake Phalen (T8)	80 ± 4	(7 ± 1) x 10^{-2}	(3.4 ± 0.4) x 10^{-6}	(7.6 ± 0.4) x 10^{-14}	(2.4 ± 0.3) x 10^{-13}	(5.7 ± 0.6) x 10^{-17}
Wastewaters						
WRRF Pre-Cl (W1)	37.1 ± 0.6	(3.0 ± 0.5) x 10^{-2}	(4.8 ± 0.4) x 10^{-5}	(7.4 ± 0.1) x 10^{-14}	(2.1 ± 0.3) x 10^{-13}	(1.7 ± 0.1) x 10^{-16}
WRRF Reuse (W2)	57.0 ± 0.9	(7.7 ± 0.3) x 10^{-2}	(1.0 ± 0.1) x 10^{-4}	(5.2 ± 0.1) x 10^{-14}	(2.6 ± 0.2) x 10^{-13}	(1.6 ± 0.2) x 10^{-16}
WRRF Post-Cl (W3)	37.5 ± 0.4	(5.8 ± 0.8) x 10^{-2}	(4.2 ± 0.3) x 10^{-5}	(1.1 ± 0.1) x 10^{-13}	(3.0 ± 0.4) x 10^{-13}	(2.0 ± 0.2) x 10^{-16}
Nine Springs Pre-UV (W4)	29.0 ± 0.8	(3.4 ± 0.1) x 10^{-2}	(5.3 ± 0.4) x 10^{-5}	(7.7 ± 0.2) x 10^{-14}	(3.8 ± 0.1) x 10^{-13}	(2.3 ± 0.2) x 10^{-16}
Nine Springs Post-UV (W5)	43.7 ± 0.5	(3.9 ± 0.1) x 10^{-2}	(3.1 ± 0.1) x 10^{-5}	(7.2 ± 0.1) x 10^{-14}	(4.3 ± 0.1) x 10^{-13}	(1.2 ± 0.1) x 10^{-16}
WLSSD Influent (W6)	17 ± 1	(1.1 ± 0.1) x 10^{-2}	NA	(4.4 ± 0.2) x 10^{-14}	(4.0 ± 0.1) x 10^{-13}	NA
WLSSD Effluent (W7)	22.5 ± 0.1	(1.6 ± 0.1) x 10^{-2}	NA	(2.8 ± 0.1) x 10^{-14}	(4.7 ± 0.1) x 10^{-13}	NA
WLSSD Pre-Cl (W8)	21.0 ± 0.9	(2.0 ± 0.1) x 10^{-2}	(1.5 ± 0.1) x 10^{-4}	(2.9 ± 0.1) x 10^{-14}	(1.3 ± 0.1) x 10^{-12}	(3.7 ± 0.1) x 10^{-16}
WLSSD Post-Cl (W9)	19.1 ± 0.7	(2.0 ± 0.1) x 10^{-2}	(6.1 ± 0.1) x 10^{-4}	(3.2 ± 0.1) x 10^{-14}	(1.2 ± 0.1) x 10^{-12}	(1.9 ± 0.1) x 10^{-16}
Metro WWTP Pre-Cl (W10)	26.9 ± 0.6	(8.9 ± 0.1) x 10^{-2}	(1.1 ± 0.1) x 10^{-3}	(4.8 ± 0.1) x 10^{-14}	(6.9 ± 0.1) x 10^{-13}	(3.3 ± 0.1) x 10^{-15}
Metro WWTP Post-Cl (W11)	34.3 ± 0.1	(7.0 ± 0.2) x 10^{-2}	(1.0 ± 0.1) x 10^{-3}	(4.6 ± 0.1) x 10^{-14}	(5.2 ± 0.1) x 10^{-13}	(2.4 ± 0.1) x 10^{-15}
Eagles Point Pre-UV (W12)	21 ± 1	(2.6 ± 0.2) x 10^{-2}	(2.5 ± 0.1) x 10^{-4}	(3.6 ± 0.2) x 10^{-14}	(2.2 ± 0.2) x 10^{-13}	(7.6 ± 0.1) x 10^{-16}
Eagles Point Post-UV (W13)	24.0 ± 0.4	(2.8 ± 0.1) x 10^{-2}	(4.0 ± 0.2) x 10^{-4}	(3.4 ± 0.1) x 10^{-14}	(2.4 ± 0.1) x 10^{-13}	(1.0 ± 0.1) x 10^{-15}

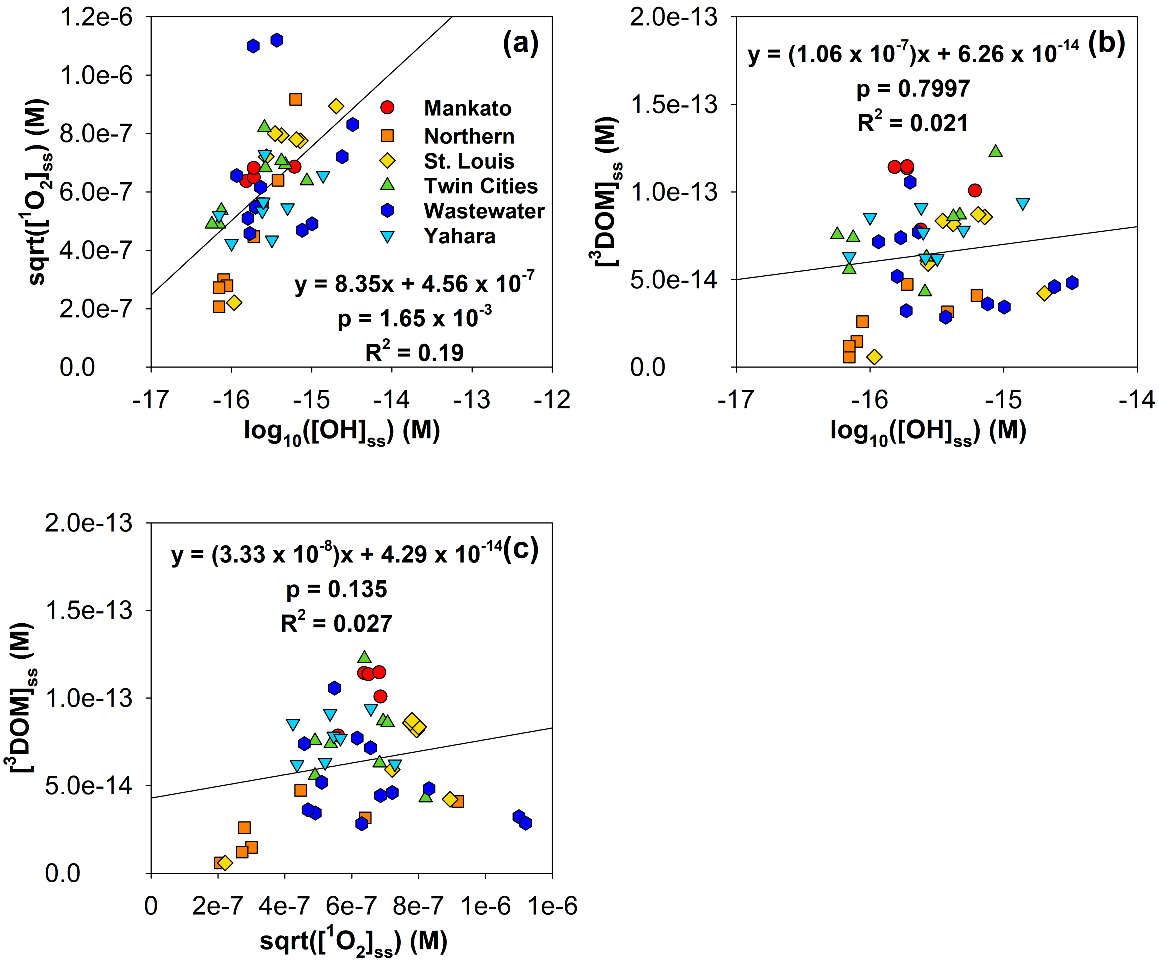

Figure S1. Linear regression analysis for (a) $[^1O_2]_{ss}$ plotted against $[^{\bullet}OH]_{ss}$, (b) $[^3DOM]_{ss}$ plotted against $[^{\bullet}OH]_{ss}$, and (c)) $[^3DOM]_{ss}$ plotted against $[^1O_2]_{ss}$. $[^1O_2]_{ss}$ and $[^{\bullet}OH]_{ss}$ were transformed by taking the square root and log value, respectively, to achieve a normal distribution.

Section S6: Contaminant kinetics experiments

Experimental procedures. Solutions of atorvastatin, benzotriazole, carbamazepine, and sulfadiazine (**Figure S2**) in each water sample were prepared to achieve a concentration of 10 µM. Solutions were then irradiated in a Luzchem photoreactor (University of St. Thomas) equipped with 16 UVA bulbs (365 nm), which is similar to the light spectrum of the Rayonet reactor (University of Wisconsin-Madison). Aliquots were removed at four time points. Atorvastatin was irradiated for 1 hour and had 15-minute time points. Sulfadiazine was irradiated for 2 hours and had 30-minute time points. Benzotriazole and carbamazepine were irradiated for 48 hours and had four time points spread throughout the 48-hour period. After irradiation, samples were analyzed using HPLC to determine rate constants of degradation assuming pseudo-first order kinetics. Specifics of HPLC methods for each contaminant are provided in **Table S7**.

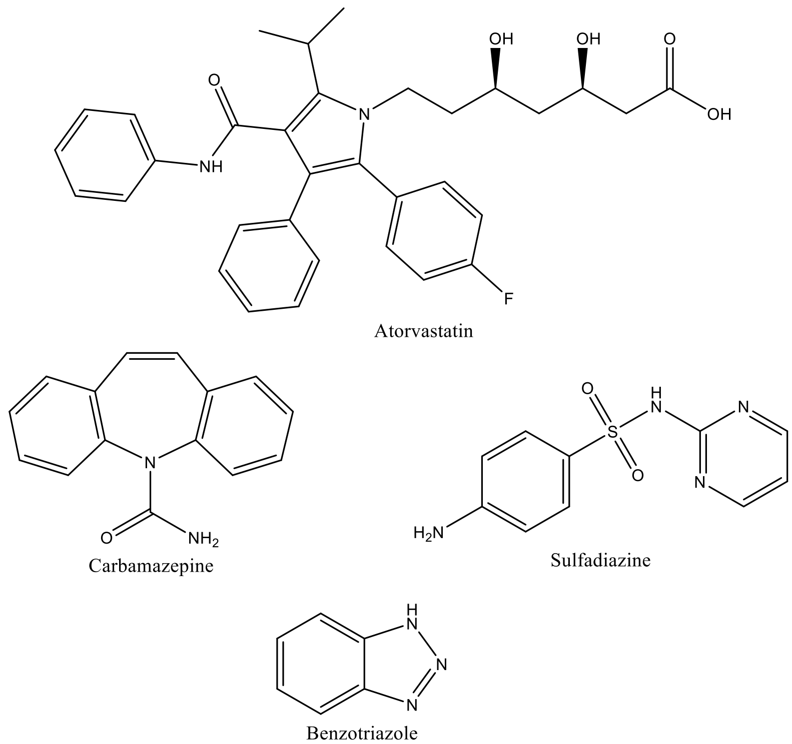

Figure S2. Chemical structures of atorvastatin, carbamazepine, sulfadiazine, and benzotriazole.

Table S7. HPLC methods used to quantify the four contaminants analyzed in this study.

Atorvastatin	
Duration	6.5 min
Pump settings	1 mL/min flow rate 0 min: 50% pH 3 phosphate buffer, 50% ACN 4 min: 40% pH 3 phosphate buffer, 60 % ACN 5 min: 70% pH 3 phosphate buffer, 30% ACN
Column	Agilent Eclipse XDB-C18 4.6 x 150 mm, 5 μm packing
Elution time	4.6 min
Wavelength	244 nm
Benzotriazole	
Duration	6.0 min

Pump settings	0.75 mL/min flow rate Isocratic: 40% HPLC water, 60% ACN
Column	Ascentis RP-Amide 25 cm x 4.6 mm, 5 μm packing
Elution time	5.5 min
Wavelength	275 nm
Carbamazepine	
Duration	5 min
Pump settings	1.0 mL/min flow rate Isocratic: 60% HPLC water, 40% ACN
Column	Agilent Eclipse XDB-C18 4.6x150mm, 5 μm packing
Elution time	3.0 min
Wavelength	282 nm
Sulfadiazine	
Duration	4.5 min
Pump settings	1.0 mL/min flow rate Isocratic: 90% pH 4 acetate buffer, 10% ACN
Injection volume	25 μL
Column	Agilent Eclipse XDB-C18 4.6x150mm, 5 μm packing
Elution time	3.2 min
Wavelength	261 nm

Light screening. All rate constants were adjusted to correct for light screening using the screening factor from equation S4 (S_λ), light intensity from equation S6 (I), and the observed rate constants (k_{obs}), to yield a screening corrected observed rate constant ($k_{obs,\ corr}$):

$$k_{obs,corr} = \frac{k_{obs}}{S_\lambda I_\lambda / I_{total}} \quad \text{(S10)}$$

where I_{total} is the summation of light intensities at wavelengths 325 – 405 nm.

Table S8. Indirect rate constants for the four contaminants in all waters.

Sample	$k_{indirect,\ atorvastatin}$ (hr^{-1})	$k_{indirect,\ carbamazepine}$ (hr^{-1})	$k_{indirect,\ sulfadiazine}$ (hr^{-1})	$k_{indirect,\ benzotriazole}$ (hr^{-1})
Northern Lakes				
Crystal Bog (N1)	(6.34 ± 0.40) x 10^{-1}	(1.11 ± 0.32) x 10^{-3}	(3.11 ± 0.58) x 10^{-2}	(1.82 ± 0.96) x 10^{-3}
Trout Bog (N2)	(4.90 ± 0.34) x 10^{-1}	(2.51 ± 0.30) x 10^{-3}	(1.66 ± 0.46) x 10^{-2}	(9.45 ± 0.12) x 10^{-3}
Allequash Lake (N3)	(5.12 ± 0.38) x 10^{-1}	(2.30 ± 0.50) x 10^{-3}	(9.75 ± 4.99) x 10^{-3}	0

Big Muskellunge Lake (N4)	(6.75 ± 2.70) x 10^{-2}	(6.41 ± 2.63) x 10^{-4}	(1.02 ± 0.18) x 10^{-1}	0
Crystal Lake (N5)	(4.16 ± 2.75) x 10^{--2}	(1.80 ± 2.48) x 10^{-4}	(1.45 ± 2.79) x 10^{-2}	0
Sparkling Lake (N6)	(3.90 ± 0.33) x 10^{-1}	(2.00 ± 0.37) x 10^{-3}	(4.54 ± 0.66) x 10^{-2}	0
Trout Lake (N7)	(8.69 ± 2.42) x 10^{-2}	(9.05 ± 2.52) x 10^{-4}	(3.32 ± 0.72) x 10^{-2}	0
Mankato				
Memories (M1)	(6.10 ± 0.27) x 10^{-1}	(7.96 ± 0.36) x 10^{-3}	(9.88 ± 0.63) x 10^{-2}	(1.76 ± 0.99) x 10^{-3}
Olsen Ditch (M2)	(5.49 ± 0.48) x 10^{-1}	(8.04 ± 0.29) x 10^{-3}	(2.69 ± 0.06) x 10^{-1}	(0.37 ± 1.01) x 10^{-3}
Wammer Ditch (M3)	(5.98 ± 0.30) x 10^{-1}	(6.74 ± 0.30) x 10^{-3}	(8.32 ± 0.70) x 10^{-2}	0
Seven-mile Creek (M4)	(7.21 ± 0.36) x 10^{-1}	(9.34 ± 0.36) x 10^{-3}	(7.63 ± 0.61) x 10^{-2}	(2.10 ± 1.08) x 10^{-3}
Kiwannis (M5)	(6.60 ± 0.26) x 10^{-1}	(8.55 ± 0.40) x 10^{-3}	(8.45 ± 1.17) x 10^{-2}	(1.76 ± 0.99) x 10^{-3}
Yahara				
North Yahara (Y1)	(6.56 ± 0.29) x 10^{-1}	(6.40 ± 0.32) x 10^{-3}	(3.26 ± 0.90) x 10^{-2}	(3.39 ± 0.99) x 10^{-3}
Lake Mendota (Y2)	(3.19 ± 0.25) x 10^{-1}	(3.33 ± 0.35) x 10^{-3}	(1.14 ± 0.31) x 10^{-1}	0
Lake Wingra (Y3)	(4.27 ± 0.26) x 10^{-1}	(4.78 ± 0.27) x 10^{-3}	(5.87 ± 0.33) x 10^{-2}	(0.43 ± 1.02) x 10^{-3}
Lake Kegonsa (Y4)	(4.69 ± 0.28) x 10^{-1}	(8.33 ± 6.70) x 10^{-3}	(1.12 ± 0.03) x 10^{-1}	(5.90 ± 1.14) x 10^{-3}
South Yahara (Y5)	(4.39 ± 0.31) x 10^{-1}	(5.07 ± 0.29) x 10^{-3}	(1.08 ± 0.05) x 10^{-1}	(0.80 ± 9.95) x 10^{-4}
Badfish Upstream (Y6)	(4.27 ± 0.28) x 10^{-1}	(5.28 ± 0.23) x 10^{-3}	(1.08 ± 0.09) x 10^{-1}	(1.37 ± 0.96) x 10^{-3}
Badfish Downstream (Y7)	(4.90 ± 0.27) x 10^{-1}	(7.31 ± 0.40) x 10^{-3}	(2.22 ± 0.65) x 10^{-2}	(2.79 ± 1.05) x 10^{-3}
Confluence (Y8)	(4.18 ± 0.28) x 10^{-1}	(4.25 ± 0.37) x 10^{-3}	(7.53 ± 0.61) x 10^{-2}	0
St. Louis River				
Sand Creek (S1)	(14.25 ± 0.30) x 10^{-1}	(9.54 ± 0.41) x 10^{-3}	(1.03 ± 0.06) x 10^{-1}	(1.31 ± 0.34) x 10^{-2}
Meadowlands (S2)	(10.77 ± 0.25) x 10^{-1}	(9.45 ± 0.23) x 10^{-3}	(4.19 ± 0.31) x 10^{-2}	(3.56 ± 1.15) x 10^{-3}
River Inn (S3)	(10.32 ± 0.24) x 10^{-1}	(8.19 ± 0.29) x 10^{-3}	(3.59 ± 0.34) x 10^{-2}	(4.74 ± 1.05) x 10^{-3}
Munger Landing (S4)	(10.12 ± 0.23) x 10^{-1}	(8.18 ± 0.28) x 10^{-3}	(3.85 ± 0.47) x 10^{-2}	(2.55 ± 1.09) x 10^{-3}
East Detroit (S5)	(9.85 ± 0.32) x 10^{-1}	(7.54 ± 0.46) x 10^{-3}	(4.25 ± 0.28) x 10^{-2}	(2.84 ± 1.10) x 10^{-3}
Blatnik Bridge (S6)	(7.68 ± 0.26)	(6.76 ± 0.42)	(1.67 ± 0.69)	(1.09 ± 1.15)

	x 10^{-1}	x 10^{-3}	x 10^{-2}	x 10^{-3}
Wisconsin Point (S7)	(5.86 ± 2.62) x 10^{-2}	(8.46 ± 2.33) x 10^{-4}	(4.89 ± 0.40) x 10^{-2}	0
Twin Cities				
River Front Park (T1)	(7.42 ± 0.25) x 10^{-1}	(8.30 ± 0.32) x 10^{-3}	(7.62 ± 0.35) x 10^{-2}	(1.39 ± 0.99) x 10^{-3}
East River Parkway (T2)	(7.25 ± 0.23) x 10^{-1}	(8.09 ± 0.35) x 10^{-3}	(5.37 ± 0.41) x 10^{-2}	(8.85 ± 9.57) x 10^{-4}
Minnesota River (T3)	(6.40 ± 0.25) x 10^{-1}	(9.38 ± 0.34) x 10^{-3}	(1.59 ± 0.08) x 10^{-1}	(1.86 ± 1.00) x 10^{-3}
Metro Downstream (T4)	(6.83 ± 0.26) x 10^{-1}	(8.31 ± 0.55) x 10^{-3}	(5.15 ± 0.31) x 10^{-2}	(1.47 ± 0.98) x 10^{-3}
Eagles Point Downstream (T5)	(6.94 ± 0.51) x 10^{-1}	(7.78 ± 0.59) x 10^{-3}	(6.45 ± 0.04) x 10^{-2}	(0.52 ± 1.11) x 10^{-3}
Lake of the Isles (T6)	(3.77 ± 0.26) x 10^{-1}	(5.43 ± 0.26) x 10^{-3}	(6.30 ± 0.59) x 10^{-2}	0
Vadnais Lake (T7)	(4.67 ± 0.23) x 10^{-1}	(5.61 ± 0.28) x 10^{-3}	(1.08 ± 0.03) x 10^{-1}	(0.54 ± 1.03) x 10^{-3}
Lake Phalen (T8)	(4.49 ± 0.25) x 10^{-1}	(8.01 ± 0.33) x 10^{-3}	(1.51 ± 0.06) x 10^{-1}	0
Wastewaters				
WRRF Pre-Cl (W1)	(5.18 ± 0.33) x 10^{-1}	(6.91 ± 0.28) x 10^{-3}	(6.32 ± 0.32) x 10^{-2}	(4.11 ± 1.01) x 10^{-3}
WRRF Reuse (W2)	(5.19 ± 0.23) x 10^{-1}	(7.57 ± 0.34) x 10^{-3}	(8.27 ± 1.24) x 10^{-2}	(2.80 ± 0.97) x 10^{-3}
WRRF Post-Cl (W3)	(5.85 ± 0.24) x 10^{-1}	(10.47 ± 0.56) x 10^{-3}	(1.57 ± 0.12) x 10^{-1}	(3.52 ± 1.01) x 10^{-3}
Nine Springs Pre-UV (W4)	(4.37 ± 0.96) x 10^{-1}	(7.87± 0.24) x 10^{-3}	(1.46 ± 0.27) x 10^{-2}	(2.46 ± 1.05) x 10^{-3}
Nine Springs Post-UV (W5)	(4.57 ± 0.23) x 10^{-1}	(7.58 ± 0.31) x 10^{-3}	(1.70 ± 0.66) x 10^{-2}	(2.35 ± 1.00) x 10^{-3}
WLSSD Influent (W6)	(5.74 ± 0.24) x 10^{-1}	(4.73 ± 0.33) x 10^{-3}	0	(2.02 ± 1.00) x 10^{-3}
WLSSD Effluent (W7)	(6.05 ± 0.27) x 10^{-1}	(6.53 ± 0.33) x 10^{-3}	0	(1.35 ± 0.15) x 10^{-2}
WLSSD Pre-Cl (W8)	(12.36 ± 0.33) x 10^{-1}	(26.45 ± 0.35) x 10^{-3}	(1.76 ± 0.35) x 10^{-2}	(3.09 ± 0.96) x 10^{-3}
WLSSD Post-Cl (W9)	(12.21 ± 0.26) x 10^{-1}	(26.40 ± 0.31) x 10^{-3}	(9.64 ± 3.58) x 10^{-3}	(2.84 ± 1.09) x 10^{-3}
Metro WWTP Pre-Cl (W10)	(4.36 ± 0.29) x 10^{-1}	(8.98 ± 0.43) x 10^{-3}	(1.53 ± 0.07) x 10^{-1}	(3.25 ± 0.97) x 10^{-3}
Metro WWTP Post-Cl (W11)	(7.43 ± 0.28) x 10^{-1}	(10.31 ± 0.47) x 10^{-3}	(7.28 ± 0.53) x 10^{-2}	(3.39 ± 0.11) x 10^{-2}
Eagles Point Pre-UV (W12)	(2.66 ± 0.23) x 10^{-1}	(6.98 ± 0.48) x 10^{-3}	0	(7.76 ± 1.13) x 10^{-3}
Eagles Point Post-UV (W13)	(2.64 ± 0.26) x 10^{-1}	(7.56 ± 0.32) x 10^{-3}	0	(2.87 ± 1.12) x 10^{-3}

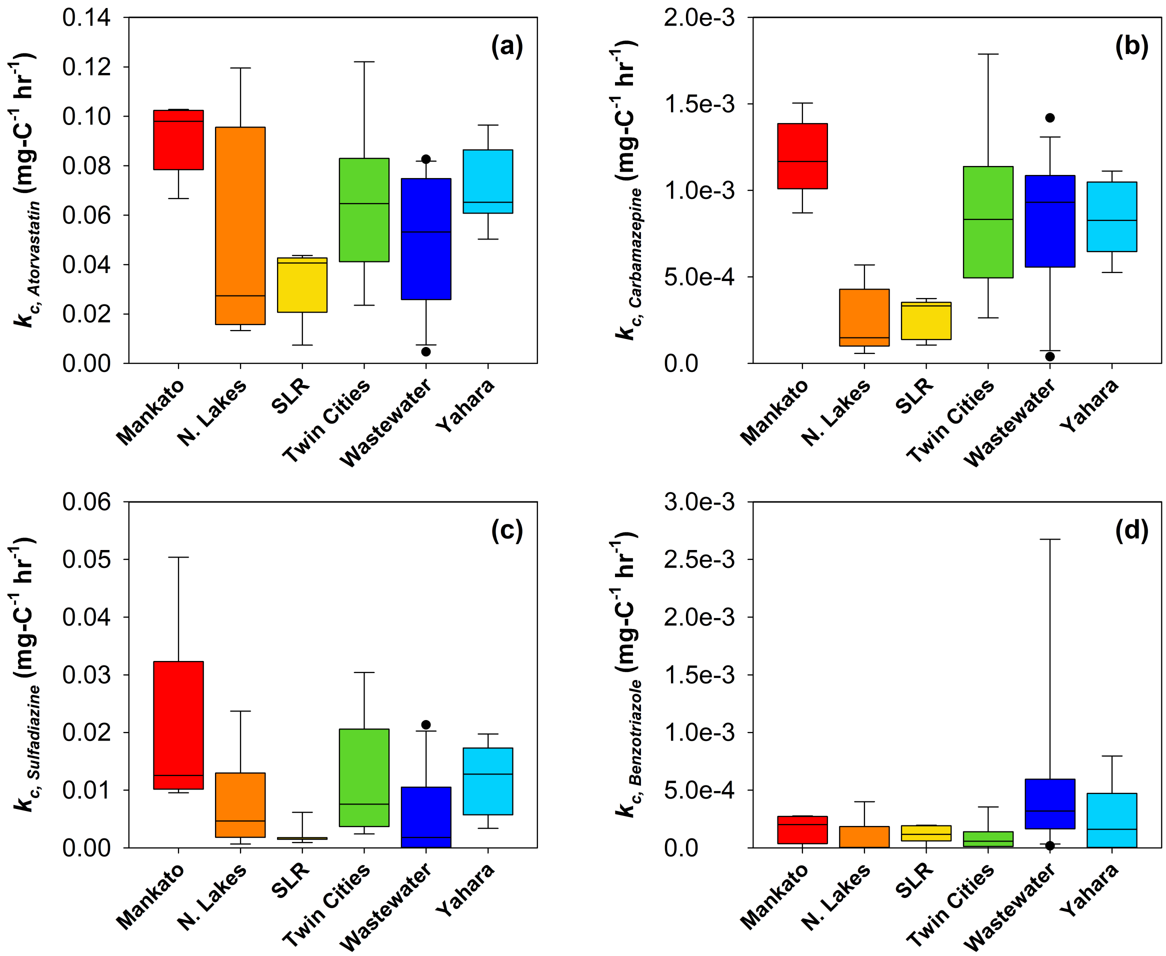

Figure S3. Indirect carbon-normalized rate constants (k_C) for (a) atorvastatin, (b) carbamazepine, (c) sulfadiazine, and (d) benzotriazole in samples collected from Mankato (n = 5), Northern Lakes (N. Lakes; n = 7), St. Louis River (SLR; n = 7), Twin Cities (n = 8), wastewater (n = 13), and the Yahara watershed (n = 8). Lines in the box-and-whisker plots represent the first and third quartiles. The line within each box represents the median. Whiskers represent minimum and maximum concentrations. Solid points represent outliers (i.e., any point less than the lower quartile or greater than the upper quartile by more than 1.5 times the interquartile range).

Table S9. Carbon-normalized indirect rate constants for the four contaminants in all waters. Values of zero represent samples where degradation was faster in the direct controls.

Sample	$k_{C,atorvastatin}$ **(hr^{-1}mg-C^{-1})**	$k_{C,carbamazepine}$ **(hr^{-1}mg-C^{-1})**	$k_{C,sulfadiazine}$ **(hr^{-1}mg-C^{-1})**	$k_{C,benzotriazole}$ **(hr^{-1}mg-C^{-1})**
Northern Lakes				
Crystal Bog (N1)	(5.84 ± 0.37) x 10^{-2}	(1.07 ± 0.30) x 10^{-4}	(3.00 ± 0.56) x 10^{-3}	(1.84 ± 0.97) x 10^{-4}
Trout Bog (N2)	(1.86 ± 0.15) x 10^{-2}	(1.01 ± 0.12) x 10^{-4}	(6.71 ± 1.85) x 10^{-4}	(4.00 ± 0.52) x 10^{-4}

Allequash Lake (N3)	(9.02 ± 0.73) x 10^{-2}	(4.29 ± 0.94) x 10^{-4}	(1.82 ± 0.93) x 10^{-3}	0
Big Muskellunge Lake (N4)	(1.57 ± 0.63) x 10^{-2}	(1.50 ± 0.61) x 10^{-4}	(2.37 ± 0.43) x 10^{-2}	0
Crystal Lake (N5)	(1.34 ± 0.88) x 10^{-2}	(5.78 ± 7.99) x 10^{-5}	(4.65 ± 8.96) x 10^{-3}	0
Sparkling Lake (N6)	(1.20 ± 0.09) x 10^{-1}	(5.70 ± 1.04) x 10^{-4}	(1.30 ± 0.19) x 10^{-2}	0
Trout Lake (N7)	(2.74 ± 0.76) x 10^{-2}	(2.85 ± 0.79) x 10^{-4}	(1.05 ± 0.23) x 10^{-2}	0
Mankato				
Memories (M1)	(6.67 ± 0.30) x 10^{-2}	(8.71 ± 0.40) x 10^{-4}	(1.08 ± 0.07) x 10^{-2}	(2.02 ± 1.14) x 10^{-4}
Olsen Ditch (M2)	(1.03 ± 0.09) x 10^{-1}	(1.51 ± 0.06) x 10^{-3}	(5.04 ± 0.11) x 10^{-2}	(0.73 ± 1.99) x 10^{-4}
Wammer Ditch (M3)	(1.02 ± 0.05) x 10^{-1}	(1.15 ± 0.05) x 10^{-3}	(1.42 ± 0.12) x 10^{-2}	0
Seven-mile Creek (M4)	(9.01 ± 0.45) x 10^{-2}	(1.17 ± 0.05) x 10^{-3}	(9.54 ± 0.77) x 10^{-3}	(2.76 ± 1.42) x 10^{-4}
Kiwannis (M5)	(9.80 ± 0.39) x 10^{-2}	(1.27 ± 0.06) x 10^{-3}	(1.25 ± 0.17) x 10^{-2}	(2.67 ± 1.54) x 10^{-4}
Yahara				
North Yahara (Y1)	(9.04 ± 0.39) x 10^{-2}	(8.82 ± 0.43) x 10^{-4}	(4.49 ± 1.24) x 10^{-3}	(4.92 ± 1.43) x 10^{-4}
Lake Mendota (Y2)	(5.03 ± 0.39) x 10^{-2}	(5.26 ± 0.55) x 10^{-4}	(1.80 ± 0.49) x 10^{-2}	0
Lake Wingra (Y3)	(6.89 ± 0.42) x 10^{-2}	(7.72 ± 0.45) x 10^{-4}	(9.46 ± 0.53) x 10^{-3}	(0.72 ± 1.72) x 10^{-4}
Lake Kegonsa (Y4)	(6.06 ± 0.36) x 10^{-2}	(1.08 ± 0.87) x 10^{-3}	(1.45 ± 0.04) x 10^{-2}	(7.97 ± 1.54) x 10^{-4}
South Yahara (Y5)	(6.15 ± 0.44) x 10^{-2}	(7.10 ± 0.41) x 10^{-4}	(1.51± 0.07) x 10^{-2}	(0.12 ± 1.46) x 10^{-4}
Badfish Upstream (Y6)	(9.64 ± 0.51) x 10^{-2}	(9.67 ± 0.43) x 10^{-4}	(1.98 ± 0.17) x 10^{-2}	(2.48 ± 1.74) x 10^{-4}
Badfish Downstream (Y7)	(7.46 ± 0.42) x 10^{-2}	(1.11 ± 0.06) x 10^{-3}	(3.37 ± 0.99) x 10^{-3}	(4.13 ± 1.56) x 10^{-4}
Confluence (Y8)	(6.15 ± 0.41) x 10^{-2}	(6.26 ± 0.54) x 10^{-4}	(1.11 ± 0.09) x 10^{-2}	0
St. Louis River				
Sand Creek (S1)	(2.07 ± 0.04) x 10^{-2}	(1.39 ± 0.06) x 10^{-4}	(1.51 ± 0.09) x 10^{-3}	(1.91 ± 0.50) x 10^{-4}
Meadowlands (S2)	(3.79 ± 0.09) x 10^{-2}	(3.32 ± 0.08) x 10^{-4}	(1.47 ± 0.11) x 10^{-3}	(1.25 ± 0.40) x 10^{-4}
River Inn (S3)	(4.26 ± 0.10) x 10^{-2}	(3.38 ± 0.12) x 10^{-4}	(1.48 ± 0.14) x 10^{-3}	(1.96 ± 0.43) x 10^{-4}
Munger Landing (S4)	(4.37 ± 0.10) x 10^{-2}	(3.53 ± 0.12) x 10^{-4}	(1.66 ± 0.20) x 10^{-3}	(1.10 ± 0.47) x 10^{-4}

East Detroit (S5)	(4.07 ± 0.13) x 10^{-2}	(3.11 ± 0.19) x 10^{-4}	(1.76 ± 0.12) x 10^{-3}	(1.17 ± 0.45) x 10^{-4}
Blatnik Bridge (S6)	(4.27 ± 0.15) x 10^{-2}	(3.75 ± 0.23) x 10^{-4}	(9.31 ± 3.86) x 10^{-4}	(6.04 ± 6.37) x 10^{-5}
Wisconsin Point (S7)	(7.39 ± 3.30) x 10^{-3}	(1.07 ± 0.29) x 10^{-4}	(6.16 ± 0.50) x 10^{-3}	0
Twin Cities				
River Front Park (T1)	(2.35 ± 0.08) x 10^{-2}	(2.64 ± 0.10) x 10^{-4}	(2.42 ± 0.11) x 10^{-3}	(4.40 ± 3.15) x 10^{-5}
East River Parkway (T2)	(4.06 ± 0.13) x 10^{-2}	(4.52 ± 0.20) x 10^{-4}	(3.00 ± 0.23) x 10^{-3}	(4.95 ± 5.35) x 10^{-5}
Minnesota River (T3)	(1.22 ± 0.05) x 10^{-1}	(1.79 ± 0.06) x 10^{-3}	(3.04 ± 0.15) x 10^{-2}	(3.55 ± 1.90) x 10^{-4}
Metro Downstream (T4)	(7.56 ± 0.28) x 10^{-2}	(9.20 ± 0.61) x 10^{-4}	(5.71 ± 0.35) x 10^{-3}	(1.63 ± 1.08) x 10^{-4}
Eagles Point Downstream (T5)	(8.54 ± 0.63) x 10^{-2}	(9.57 ± 0.72) x 10^{-4}	(7.94 ± 0.51) x 10^{-3}	(0.64 ± 1.37) x 10^{-4}
Lake of the Isles (T6)	(4.31 ± 0.29) x 10^{-2}	(6.22 ± 0.30) x 10^{-4}	(7.22 ± 0.68) x 10^{-3}	0
Vadnais Lake (T7)	(6.21 ± 0.31) x 10^{-2}	(7.46 ± 0.38) x 10^{-4}	(1.44 ± 0.04) x 10^{-2}	(0.72 ± 1.37) x 10^{-4}
Lake Phalen (T8)	(6.73 ± 0.37) x 10^{-2}	(1.20 ± 0.05) x 10^{-3}	(2.26 ± 0.09) x 10^{-2}	0
Wastewaters				
WRRF Pre-Cl (W1)	(8.07 ± 0.52) x 10^{-2}	(1.08 ± 0.04) x 10^{-3}	(9.85 ± 0.50) x 10^{-3}	(6.92 ± 1.70) x 10^{-4}
WRRF Reuse (W2)	(7.03 ± 0.32) x 10^{-2}	(1.03 ± 0.05) x 10^{-3}	(1.12 ± 0.17) x 10^{-2}	(4.28 ± 1.48) x 10^{-4}
WRRF Post-Cl (W3)	(7.93 ± 0.32) x 10^{-2}	(1.42 ± 0.08) x 10^{-3}	(2.13 ± 0.16) x 10^{-2}	(4.96 ± 1.42) x 10^{-4}
Nine Springs Pre-UV (W4)	(5.35 ± 1.18) x 10^{-2}	(9.64 ± 0.29) x 10^{-4}	(1.79 ± 0.33) x 10^{-3}	(3.17 ± 1.35) x 10^{-4}
Nine Springs Post-UV (W5)	(5.51 ± 0.27) x 10^{-2}	(9.14 ± 0.37) x 10^{-4}	(2.05 ± 0.80) x 10^{-3}	(2.99 ± 1.27) x 10^{-4}
WLSSD Influent (W6)	(4.67 ± 0.19) x 10^{-3}	(3.84 ± 0.27) x 10^{-5}	0	(1.64 ± 0.81) x 10^{-5}
WLSSD Effluent (W7)	(1.19 ± 0.05) x 10^{-2}	(1.28 ± 0.06) x 10^{-4}	0	(2.64 ± 0.29) x 10^{-4}
WLSSD Pre-Cl (W8)	(2.34 ± 0.06) x 10^{-2}	(5.01 ± 0.07) x 10^{-4}	(3.33 ± 0.66) x 10^{-4}	(5.86 ± 1.81) x 10^{-5}
WLSSD Post-Cl (W9)	(2.84 ± 0.06) x 10^{-2}	(6.14 ± 0.07) x 10^{-4}	(2.24 ± 0.83) x 10^{-4}	(6.60 ± 2.53) x 10^{-5}
Metro WWTP Pre-Cl (W10)	(5.32 ± 0.35) x 10^{-2}	(1.10 ± 0.05) x 10^{-3}	(1.86 ± 0.08) x 10^{-2}	(3.96 ± 1.19) x 10^{-4}
Metro WWTP Post-Cl (W11)	(8.26 ± 0.31) x 10^{-2}	(1.15 ± 0.05) x 10^{-3}	(8.08 ± 0.59) x 10^{-3}	(3.77 ± 0.12) x 10^{-3}

Eagles Point Pre-UV (W12)	(3.55 ± 0.30) x 10^{-2}	(9.31 ± 0.64) x 10^{-4}	0	(1.03 ± 0.15) x 10^{-3}
Eagles Point Post-UV (W13)	(2.94 ± 0.29) x 10^{-2}	(8.40 ± 0.36) x 10^{-4}	0	(3.19 ± 1.25) x 10^{-4}

Section S7: Quenching experiments

Table S10. Bimolecular reaction rate constants for quenchers and $^{\bullet}$OH.

Compound	Role	*k* (M^{-1} s^{-1})	Reference
Sorbate	^{3}DOM quencher	5.8 x 10^{9}	11
Histidine	$^{1}O_2$ quencher	5.7 x 10^{9}	12
DABCO	$^{1}O_2$ quencher	1.3 x 10^{9}	13
Isopropanol	$^{\bullet}$OH quencher	1.6 x 10^{9}	14

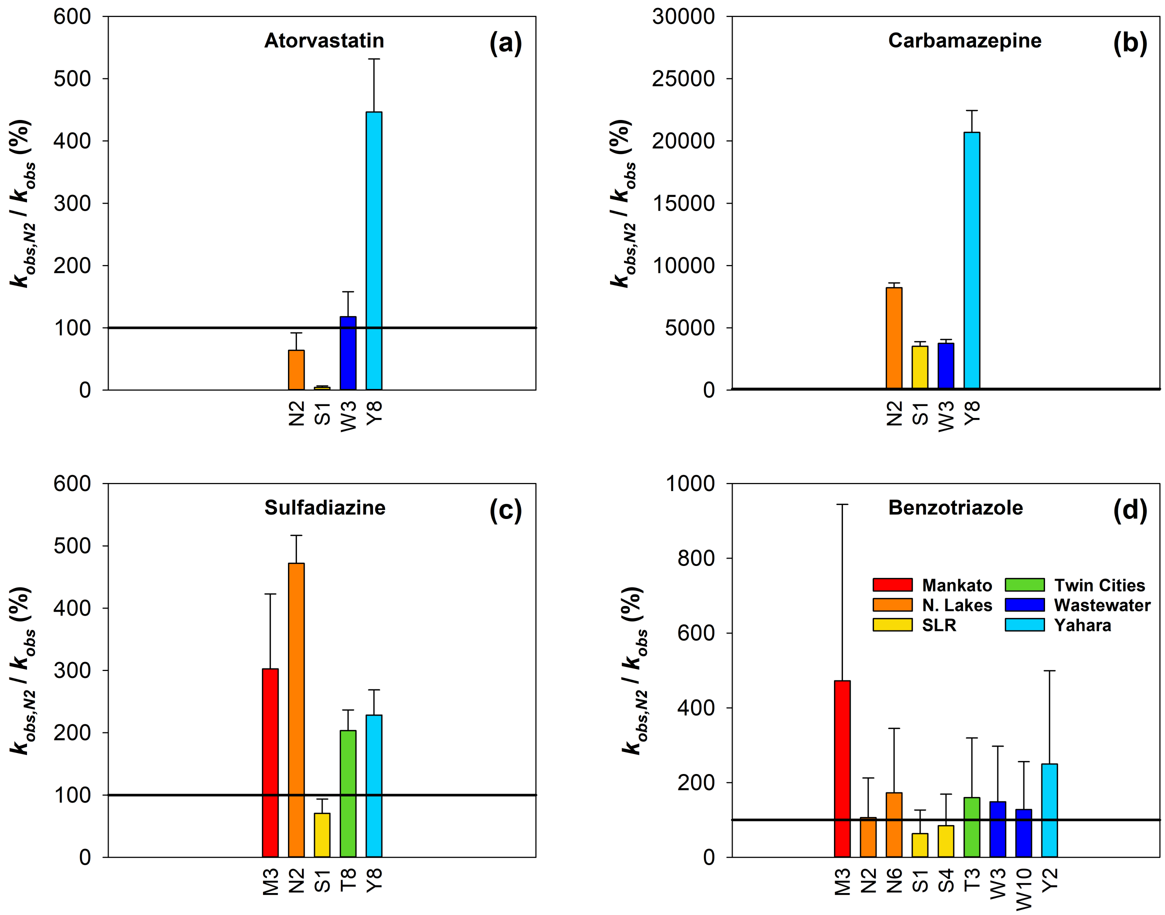

Figure S4. The relative change in observed rate constants in the nitrogen-sparged solutions compared to air-saturated samples for (a) atorvastatin, (b) carbamazepine, (c) sulfadiazine, and (d) benzotriazole. All rate constants are expressed as a percent of the observed rate constant in air-saturated samples. The solid horizontal line represents the unquenched rate (i.e., 100%). Error bars correspond to the standard deviation of triplicate measurements.

Table S11. Summary of PPRI reactivity trends determined by quencher experiments and linear regression analysis.

Compound	PPRI/ Factor	Quencher Experiments	Correlations with $k_{indirect}$	Correlations with k_C
Atorvastatin	^3DOM	Up to 44 ± 23 % due to ^3DOM; modest increase with nitrogen sparging	Positive with $[^3DOM]_{ss}$	Positive with f_{TMP}
	$^1O_2$	Up to 21 ± 22 % due to $^1O_2$	Positive with $[^1O_2]_{ss}$	Positive with Φ_{1O2}
	$^{\bullet}OH$	$^{\bullet}OH$ is minor	Positive with $[^{\bullet}OH]_{ss}$	No trend with $\Phi_{\bullet OH}$
	[DOC] or DOM composition	N/A	Positive with [DOC]	Negative with $H:C_w$, positive with DBE_w
Carbamazepine	^3DOM	Up to 90 ± 13 % due to ^3DOM; large increase due to nitrogen sparging	Positive with $[^3DOM]_{ss}$	Positive with f_{TMP}
	$^1O_2$	Up to 69 ± 32 % due to $^1O_2$	Positive with $[^1O_2]_{ss}$	Positive with Φ_{1O2}
	$^{\bullet}OH$	$^{\bullet}OH$ is minor	Positive with $[^{\bullet}OH]_{ss}$	No trend with $\Phi_{\bullet OH}$
	[DOC] or DOM composition	N/A	No trend with [DOC]	Positive with FI, negative with HIX
Sulfadiazine	^3DOM	Up to 73 ± 19 % due to ^3DOM; modest increase with nitrogen sparging	Positive with $[^3DOM]_{ss}$	Positive with f_{TMP}
	$^1O_2$	Up to 80 ± 20 % due to $^1O_2$	No trend with $[^1O_2]_{ss}$	Positive with Φ_{1O2}
	$^{\bullet}OH$	$^{\bullet}OH$ is minor	No trend with $[^{\bullet}OH]_{ss}$	Negative trend with $\Phi_{\bullet OH}$
	[DOC] or DOM composition	N/A	No trend with [DOC]	Negative with EDC, positive with $E_2:E_3$
Benzotriazole	^3DOM	Up to 64 ± 31 % due to ^3DOM; modest increase with nitrogen sparging	Negative trend with $[^3DOM]_{ss}$	No trend with f_{TMP}
	$^1O_2$	Up to 55 ± 32 % due to $^1O_2$	No trend with $[^1O_2]_{ss}$	Positive with Φ_{1O2}
	$^{\bullet}OH$	Up to 65 ± 24 % due to $^{\bullet}OH$	Positive with $[^{\bullet}OH]_{ss}$	Positive trend with $\Phi_{\bullet OH}$
	[DOC] or DOM composition	N/A	Positive with [DOC]	Positive with FI

Section S8: Linear regression analysis

Linear regression analysis was performed to correlate non-carbon normalized and carbon-normalized rate constants to aspects of water chemistry, DOM composition, and PPRI formation. Non-carbon normalized rate constants ($k_{indirect}$) were correlated with [DOC], $[^3DOM]_{ss}$, $[^1O_2]_{ss}$, and $[^\bullet OH]_{ss}$. Carbon-normalized rate constants (k_C) were correlated with $SUVA_{254}$, E_2:E_3, HIX, FI, EDC, f_{TMP}, H:C_w, O:C_w, DBE_w, Φ_{1O2}, and $\Phi_{\bullet OH}$. All data were transformed to achieve a normal distribution of values as necessary. Variables that were transformed include $k_{indirect,carbamazepine}$ (x^2), $k_{indirect,sulfadiazine}$ (sqrt(x)), $k_{indirect,benzotriazine}$ ($\log_{10}$(x)), $k_{C,sulfadiazine}$ (sqrt(x)), $k_{C,benzotriazine}$ ($\log_{10}$(x)), E_2:E_3 ($\log_{10}$(x)), HIX ($\log_{10}$(x)), FI (sqrt(x)), EDC ($\log_{10}$(x)), f_{TMP} (sqrt(x)), Φ_{1O2} (sqrt(x)), Φ_{OH} ($\log_{10}$(x)), $[^1O_2]_{ss}$ (sqrt(x)), and $[^\bullet OH]_{ss}$ ($\log_{10}$(x)). Only correlations that were statistically significant (95% confidence interval, $p < 0.05$) were included in figures.

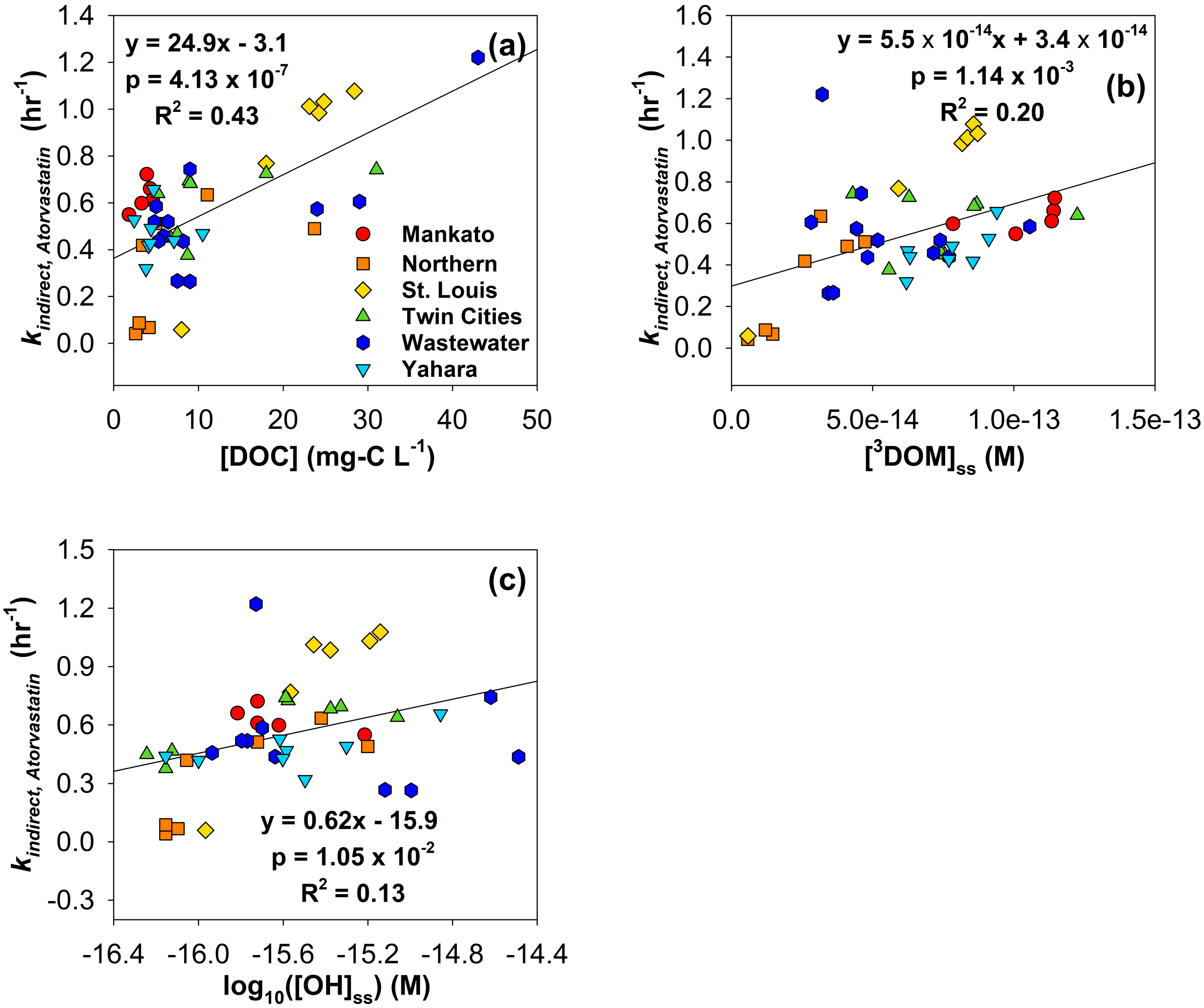

Figure S5. Linear regression analysis for $k_{indirect,Atorvastatin}$ and (a) [DOC], (b) $[^3DOM]_{ss}$, and (c) $[^{\bullet}OH]_{ss}$.

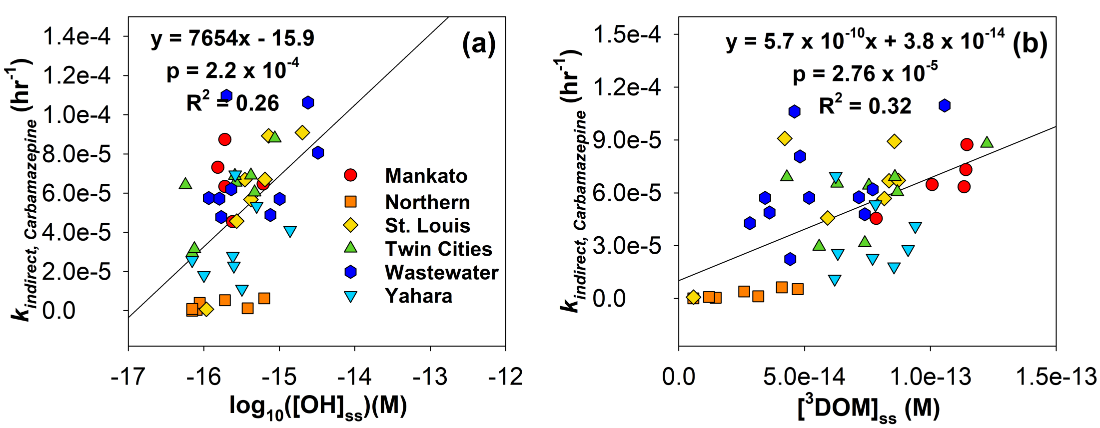

Figure S6. Linear regression analysis for $k_{indirect,\ Carbamazepine}$ and (a) $[^{\bullet}OH]_{ss}$ and (b) $[^3DOM]_{ss}$.

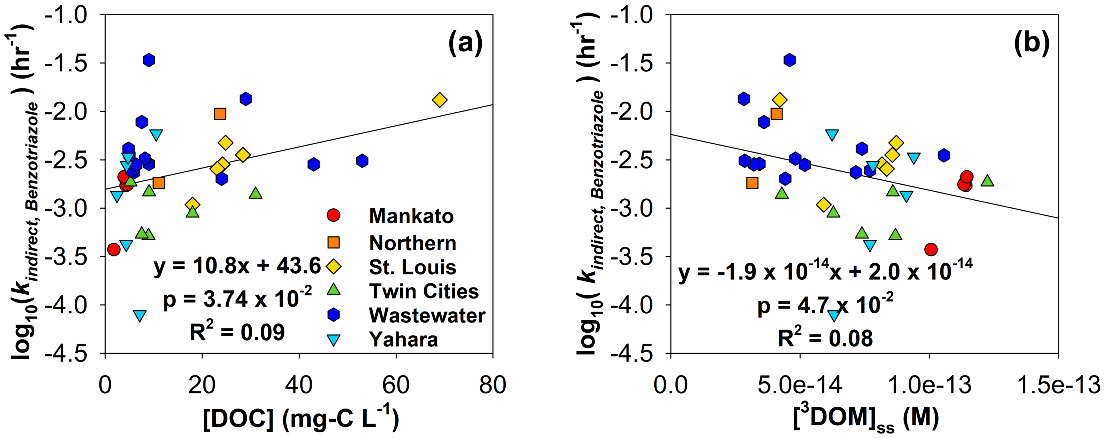

Figure S7. Linear regression analysis for $k_{indirect,\ Benzotriazine}$ and (a) [DOC] and (b) $[^3DOM]_{ss}$.

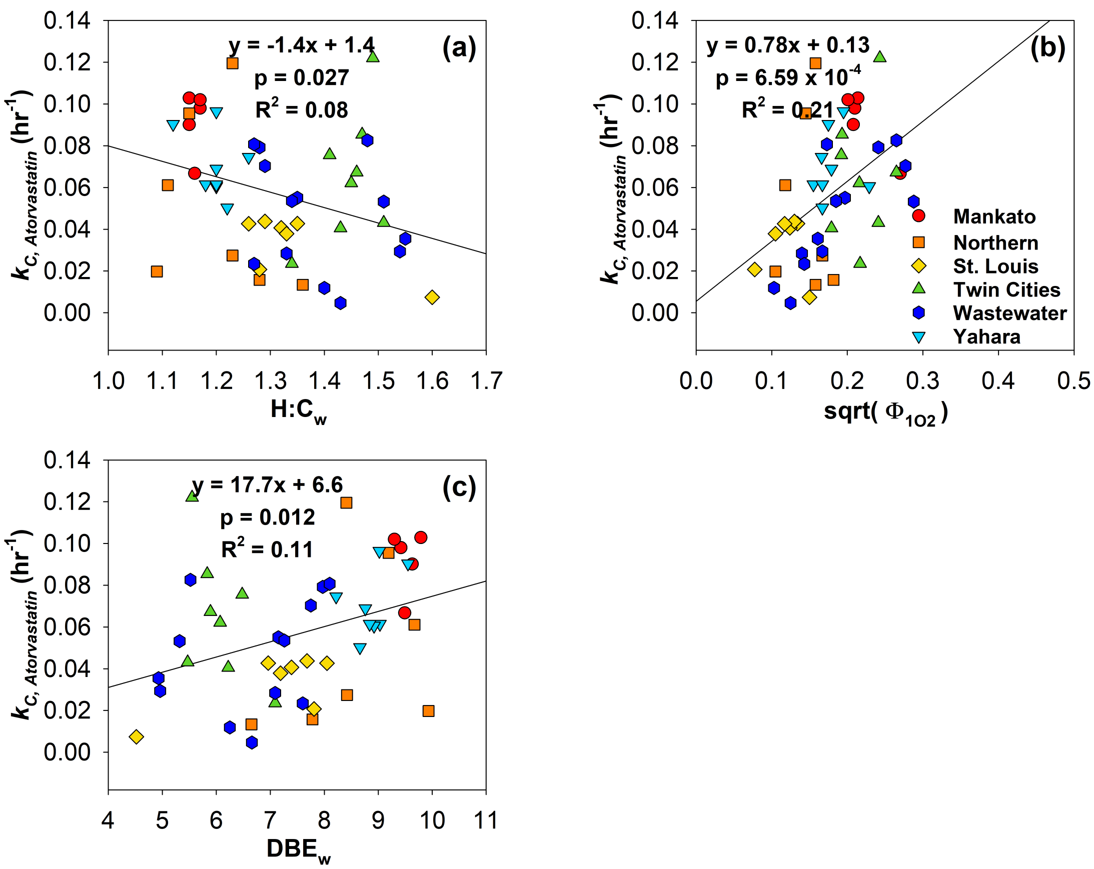

Figure S8. Linear regression analysis for $k_{C,Atorvastatin}$ and (a) H:C_w, (b) Φ_{1O2}, and (c) DBE_w.

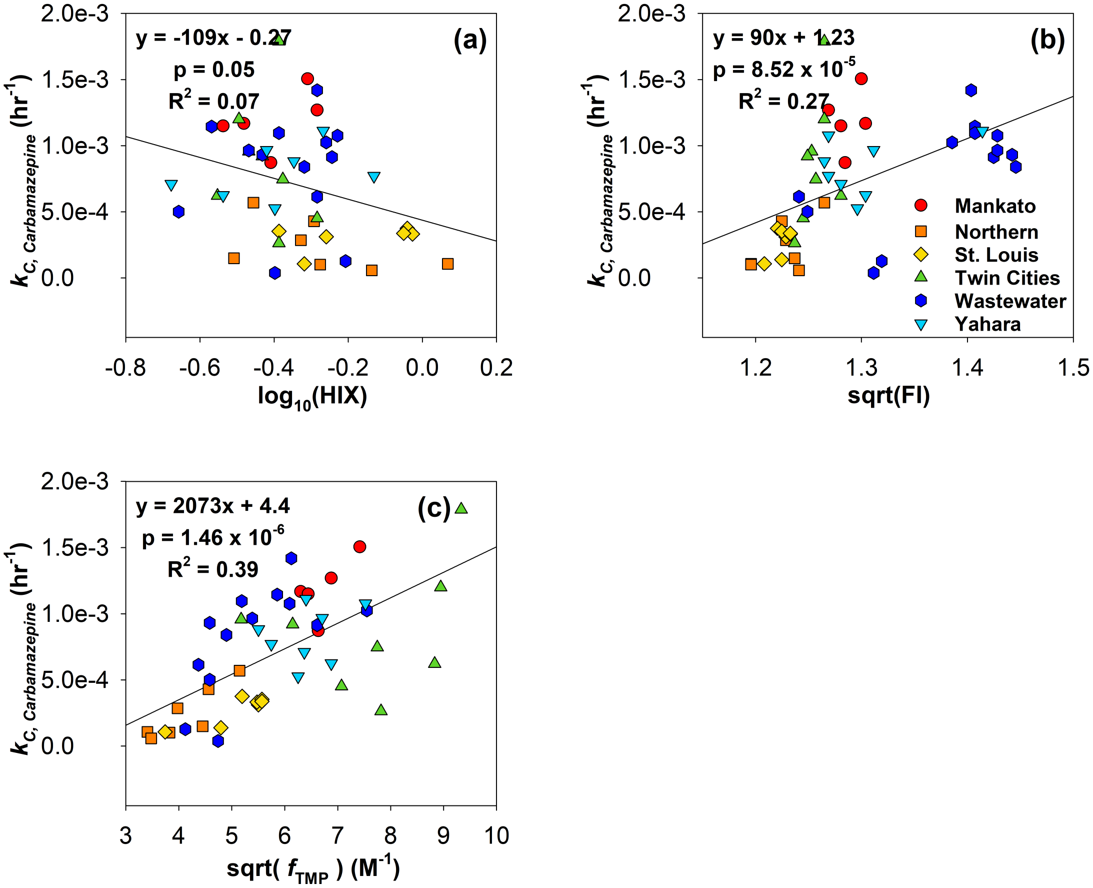

Figure S9. Linear regression analysis for $k_{C,Carbamazepine}$ and (a) HIX, (b) FI, and (c) f_{TMP}.

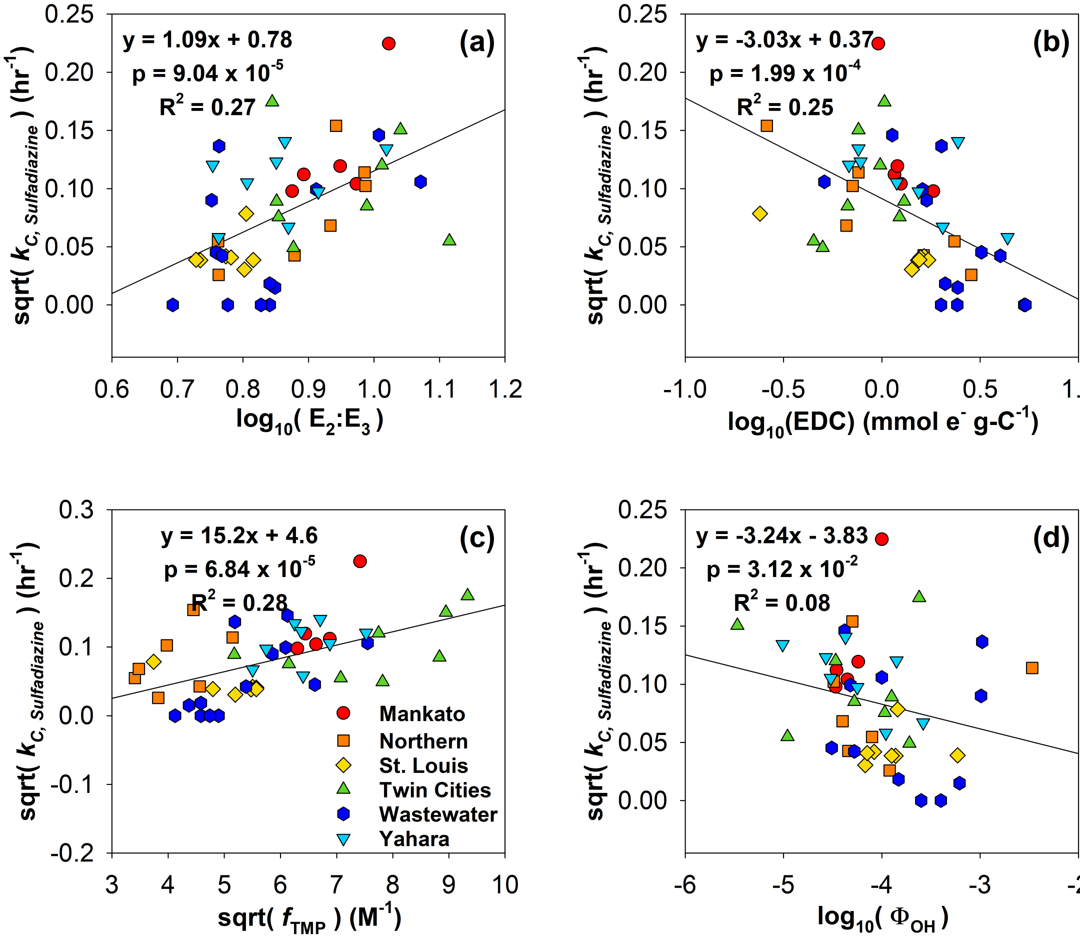

Figure S10. Linear regression analysis for $k_{C,Sulfadiazine}$ and (a) E_2:E_3, (b) EDC, (c) f_{TMP} and (d) $\Phi_{\bullet OH}$.

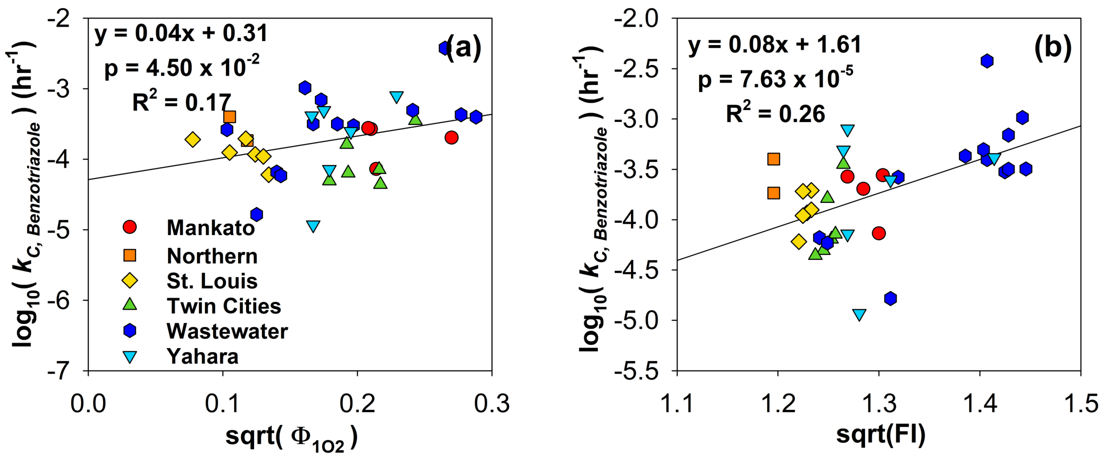

Figure S11. Linear regression analysis for $k_{C,Benzotriazole}$ and (a) Φ_{1O2} and (b) fluorescence index.

Section S9: References

(1) Wang, D.; Bolton, J. R.; Hofmann, R. Medium pressure UV Combined with chlorine advanced oxidation for trichloroethylene destruction in a model water. *Water Res.* **2012**, *46* (15), 4677–4686.

(2) Berg, S. M.; Wammer, K. H.; Remucal, C. K. Dissolved organic matter photoreactivity is determined by its optical properties, redox activity, and molecular composition. *Environ. Sci. Technol.* **2023** *57* (16), 6703-6711.

(3) Maizel, A. C.; Remucal, C. K. The effect of probe choice and solution conditions on the apparent photoreactivity of dissolved organic matter. *Environ. Sci. Process. Impacts* **2017**, *19* (8), 1040–1050.

(4) Maizel, A. C.; Remucal, C. K. Molecular composition and photochemical reactivity of size-fractionated dissolved organic matter. *Environ. Sci. Technol.* **2017**, *51* (4), 2113–2123.

(5) Appiani, E.; Ossola, R.; E. Latch, D.; R. Erickson, P.; McNeill, K. Aqueous singlet oxygen reaction kinetics of furfuryl alcohol: Effect of temperature, pH, and salt content. *Environ. Sci. Process. Impacts* **2017**, *19* (4), 507–516.

(6) Page, S. E.; Arnold, W. A.; McNeill, K. Terephthalate as a probe for photochemically generated hydroxyl radical. *J. Environ. Monit.* **2010**, *12* (9), 1658–1665.

(7) Laszakovits, J. R.; Berg, S. M.; Anderson, B. G.; O'Brien, J. E.; Wammer, K. H.; Sharpless, C. M. *p*-Nitroanisole/pyridine and *p*-nitroacetophenone/pyridine actinometers revisited: Quantum yield in comparison to ferrioxalate. *Environ. Sci. Technol. Lett.* 2017, *4* (1), 11–14.

8) Maizel, A. C.; Li, J.; Remucal, C. K. Relationships between dissolved organic matter composition and photochemistry in lakes of diverse trophic status. *Environ. Sci. Technol.* **2017**, *51* (17), 9624–9632.

(9) Jasper, J. T.; Sedlak, D. L. Phototransformation of wastewater-derived trace organic contaminants in open-water unit process treatment wetlands. *Environ. Sci. Technol.* **2013**, *47* (19), 10781–10790.

(10) Westerhoff, P.; Mezyk, S. P.; Cooper, W. J.; Minakata, D. Electron pulse radiolysis determination of hydroxyl radical rate constants with Suwannee River fulvic acid and other dissolved organic matter isolates. *Environ. Sci. Technol.* **2007**, *41* (13), 4640–4646.

(11) Buxton, G. V.; Greenstock, C. L.; Helman, W. P.; Ross, A. B. Critical review of rate constants for reactions of hydrated electrons, hydrogen atoms and hydroxyl radicals ($^{\bullet}OH/^{\bullet}O^{-}$) in aqueous solution. *J. Phys. Chem. Ref. Data* **1988**, *17* (2), 513–886.

(12) Aruoma, O. I.; Laughton, M. J.; Halliwell, B. Carnosine, homocarnosine and anserine: Could they act as antioxidants in vivo? *Biochem. J.* **1989**, *264* (3), 863–869.

(13) Anderson, R. F.; Patel, K. B. The effect of 1,4-diazabicyclo[2.2.2]octane on the radiosensitivity of bacteria. *Photochem. Photobiol.* **1978**, *28* (4–5), 881–885.

(14) Motohashi, N.; Saito, Y. Competitive measurement of rate constants for hydroxyl radical reactions using radiolytic hydroxylation of benzoate. *Chem. Pharm. Bull.* **1993**, *41* (10), 1842–1845.